Journal of Hydrology: Regional Studies 47 (2023) 101379

Contents lists available at ScienceDirect

Journal of Hydrology: Regional Studies

journal homepage: www.elsevier.com/locate/ejrh

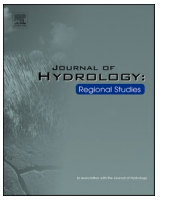

Factors controlling the changes in surface water temperature in the Ebro River Basin

M.A. Lorenzo-González [*], D. Quílez, D. Isidoro [1]

Departamento de Sistemas Agrícolas, Forestales y Medio Ambiente, Centro de Investigación y Tecnología Agroalimentaria de Aragón (CITA), Gobierno de Aragón, Avda. Montañana 930, 50059 Zaragoza, Spain

ARTICLE INFO

Keywords:
Water temperature
Annual cycle
Trends
Natural factors
Anthropogenic affections
Nuclear power plants
Reservoirs
Irrigation

ABSTRACT

Study region: The Ebro River Basin, northeast Spain.
Study focus: The work analyzes the evolution of water temperature (T_w) in the Ebro River and its main tributaries, its annual cycle and its trends, as well as the effects of various natural and anthropogenic factors on them.
New hydrological insights for the region: Stations located downstream of nuclear power plants showed an anomalous increase in T_w not consistent with the river section where they are located, with higher values in the lower-flow months (August to December). The stations affected by the main reservoirs along the Ebro River showed a lower annual temperature range and the stations located in large irrigation systems showed a lower summer temperature compared to other stations with similar climatic conditions. Finally, there was a significant annual increase in T_w at all stations (mean ΔT_w=0.05 °C/year), except those located at the head of the tributaries. These trends were higher for the stations downstream of the Ascó nuclear power plant ($\Delta T_w > 0.08$ °C/year). Seasonally, the spring months showed the greatest changes, with higher increases at the stations downstream of Ascó ($\Delta T_w \geq 0.10$ °C/year). The increase in air temperature associated with global warming and the decrease in flows associated with the increase in water consumption resulted in an increase in the temperature of the river.

1. Introduction

Water temperature (T_w) is an important parameter in river systems, influencing all physical, chemical and biological processes occurring in the water (Stevens et al., 1975). It is also an important variable affecting water quality regarding industrial water supply, refrigeration systems and recreational uses. High water temperature enhances the growth of microorganisms and may increase problems due to bad taste, odor or color and corrosion problems (WHO, 2022). On the other hand, water temperature in rivers (average value, evolution through the year, and long-term trends) results from natural and anthropogenic factors. Air temperature, volume of precipitation as rainfall and snowfall, groundwater discharge and land cover are some of the natural factors, while return flows from human activities such as industrial uses – mainly refrigeration-, irrigation or climate and land use changes – are some of the anthropogenic factors.

* Corresponding author.
E-mail addresses: mlorenzo@cita-aragon.es (M.A. Lorenzo-González), dquilez@movistar.es (D. Quílez), disidoro66@unizar.es (D. Isidoro).
[1] Present address: Departamento de Métodos Estadísticos, Universidad de Zaragoza, Escuela Universitaria Politécnica de Teruel, c/Atarazana 2, 44003 Teruel, Spain.

https://doi.org/10.1016/j.ejrh.2023.101379
Received 20 December 2022; Received in revised form 16 March 2023; Accepted 6 April 2023
Available online 13 April 2023

Water temperature has a paramount influence on river ecosystems, affecting the life cycles of many organisms, their rate of growth, and metabolic or reproductive rates and interfering with the competitiveness among species (Schmidt-Nielsen, 1997; García de Jalón, 1996; García de Jalon et al., 1988; Ward and Stanford, 1982; Vannote and Sweeney, 1980; Nebeker, 1971).

Water temperature also affects water composition through its influence on mineral solubility and CO_2 partial pressure (Stumm and Morgan, 1970). An increase in T_w generally increases salt solubility and therefore water salinity (Catalán and Catalán, 1987). An analysis of the main mineral dissolution rates for the waters of the Ebro River Basin showed that T_w and air temperature (T_a), related to the CO_2 partial pressure, had a positive relationship with the number of calcite- and dolomite-saturated and oversaturated samples (Alberto and Navas, 1987). Water temperature is also a conditioning factor for water pH, with pH decreasing as T_w increases (Labrador-Páez et al., 2019). The Ebro River Basin Authority (Confederación Hidrográfica del Ebro, CHE) has monitored T_w as a possible cause of water acidification trends (CHE, 2012) and found a general upward trend in water acidification and in T_w in many control points of the rivers related to the atmospheric emissions of thermal power plants.

Dissolved oxygen (DO), an important factor for aquatic life, is determined by T_w, as cold water can hold more dissolved oxygen than warm water (Stevens et al., 1975). Higher T_w may also enhance organism metabolism, leading to enhanced oxygen consumption and decreasing DO. This alteration can contribute to anoxia events in deep rivers with low water velocity (Prats, 2011) or to the profusion of macrophytes in stretches downstream of major reservoirs, where minimum flows are quite constant (García Vera, 2013). In this regard, the CHE has implemented a water-temperature depth-profile control network throughout reservoirs in the Ebro River Basin to prevent eutrophication and to study water stratification (CHE, 2018).

Water temperature is controlled primarily by climatic and geographic factors such as annual and daily solar radiation cycles, contribution from snowmelt, or river altitude. Many of these factors, such as rainfall, temperature or snowmelt patterns, can be affected by climate variability. In general, a higher altitude entails a lower average and lower annual range of T_w (Arrúe and Alberto, 1986). Other natural drivers of T_w in a river stretch are groundwater discharge (including thermal springs), flow velocity, channel characteristics and storage capacity, riparian area, and inputs from tributaries (Poole and Berman, 2001).

Human effects on T_w are normally derived from riparian and land use changes, channel alterations, and discharges (either directly to the main stem or through tributaries). The most important anthropogenic drivers of T_w are water storage in reservoirs and river regulation (Webb, 1996; Webb and Walling, 1988); discharges from nuclear or thermal power plants (Peterson and Jaske, 1968); urban and industrial discharges (Kinouchi et al., 2007); river channeling and riparian modifications (Poole and Berman, 2001); irrigation return flows (Verma, 1986); and changes in land uses or water diversions (Beschta and Taylor, 1988).

Climate change is also an anthropogenic driver of T_w trends. It can affect T_w in a different fashion either through changes in air temperature or in precipitation (amount and intensity of the rainfall and the type of precipitation, rain or snow). During the last century, T_a increased over most of the Ebro River Basin, with an average increase of 0.2 °C per decade in the 1950–2006 period (De Castro et al., 2005) and a higher summer increase up to 0.34 °C per decade (López-Moreno et al., 2011). Land use changes also contribute to alterations in the flow regime (Gusarov, 2019; Fazel et al., 2017) and thus of T_w (Álvarez-Cabria et al., 2016).

Alterations in the natural thermal regime of rivers have been found worldwide. The European Environmental Agency (EEA) reported an increase in T_w of 1–3 °C in the major European rivers over the last century (EEA, 2017). For instance, the mean T_w increased by 1 °C in the Danube River during the last century and by 3 °C in the lower reaches of the Rhine River between 1910 and 2010. The T_w increase in the Rhine River was attributed mainly to the increase in water use for cooling, with one-third attributed to the increase in T_a as a result of climate change (EEA, 2017). The main stretch of the Danube River in Austria showed an increase of 0.8–1.0 °C in the 1901–1990 period, with the highest value, 2.0 °C, in October and November (Webb and Nobilis, 1995); part of this increase was associated with heated effluents and regulation and with the climate patterns of the North Atlantic Oscillation (Webb and Nobilis, 2007). Other studies in the USA showed an increase of 0.009–0.077 °C/year in 20 major streams and rivers (Kaushal et al., 2010), with higher trends in summer months. Seven unregulated rivers in the northwestern USA showed a summer increase of 0.22 °C per decade for the 1980–2009 period, in which the dominant driving factor was the observed increase in T_a (Isaak et al., 2011).

Except for some general studies in the 1980s (Arrúe and Alberto, 1986; Alberto and Arrúe, 1986), most studies on the T_w of the Ebro River Basin have focused either on the effects of anthropogenic alterations on T_w or on the effects of T_w on river ecosystems (Val et al., 2016; García de Jalón, 1996; García de Jalón et al., 1988). Most of the latter studies have generally addressed the effects of reservoirs and discharges from the Ascó nuclear power plant in the lower reach of the Ebro River (Arbat-Bofill et al., 2014; Prats, 2012; Prats et al., 2010; Val et al., 2003; Dolz et al., 1996). Other studies have analyzed the trends of T_w along with other water quality parameters using different statistical tools (Abaurrea et al., 2011; Valencia, 2007; Bouza, 2006) or have even developed models for the creation of T_w scenarios (Val et al., 2018).

Thus, there has been a lack of specific studies on the temporal and spatial variability of T_w in the Ebro River Basin that incorporate the river as a continuous system. The few analyses available on T_w trends did not incorporate long and complete data series (Diamantini et al., 2018; Bouza-Deaño et al., 2008). Furthermore, the Ebro River Basin Authority has been recording T_w since 1972 at the main water quality monitoring stations along the Ebro River and its main tributaries (CHE, 2021a). This 40-year-long series offers a good opportunity to analyze the behavior of T_w in a global context, including spatial distribution, seasonal patterns, and long-term trends.

The objectives of this paper are (i) to assess the thermal regime of the Ebro River and its main tributaries over a 40-year period; (ii) to establish the trends in surface water temperatures in the Ebro River Basin; and (iii) to search for patterns in the thermal regime and, especially, water temperature trends and their potential link to natural factors or anthropogenic drivers (such as water diversion, power plants cooling, urban and agricultural discharges or land use changes). This is necessarily a preliminary analysis, as it only addresses the course and main tributaries of the Ebro River (and does not incorporate long-term, detailed information on land uses and water diversion). However, it may be used as a starting point for establishing the links between climate variability, global warming and

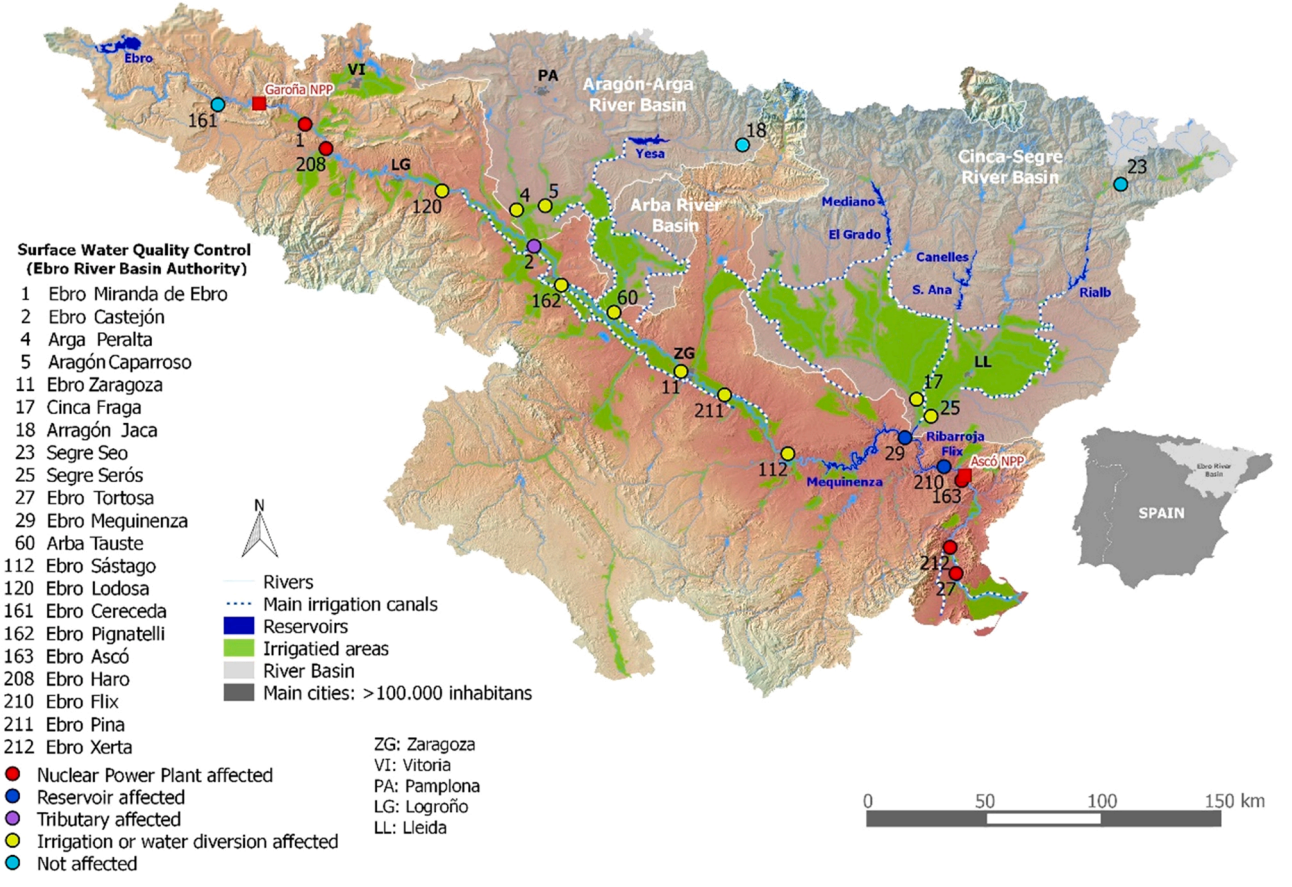

Fig. 1. Map of the Ebro River Basin with the locations of the power plants, irrigated areas, main cities, and surface water quality monitoring stations used in this work. The number is the identification code in the surface water quality network.

land use changes with T_w, providing frameworks for analyzing future scenarios of water and land use and climate change on T_w, both directly and through diminished water resources.

2. Materials and methods

2.1. Description of the study area

The Ebro River is the largest flowing river on the Iberian Peninsula, with a natural flow of 15,506 Mm^3/year (1980–2017; CHE, 2022) and a length of 950 km. It has a catchment area of 85,570 km^2 with high physiographic and climatic variability. It is located between 4°24′15″ W and 43°02′17″ N and 0°52′7″ E and 40°43′49″ N. The basin is limited to the north by the Cantabrian Mountains and the Pyrenean Range (with altitudes up to 3500 m.a.s.l.) and to the south by the Iberian Ranges (up to 2500 m.a.s.l.). These ranges and the headwater areas have an oceanic and Mediterranean mountain climate with precipitation from 800 to 2000 mm/year and a mean annual air temperature (T_a) from 9 °C to 12 °C (CHE, 2022). In contrast, the central basin area (Ebro Depression) is characterized by a dry Mediterranean-continental climate, with low and discontinuous precipitation (350–700 mm/year) and a mean annual T_a of 11–14 °C with an annual range of 17–20 °C (CHE, 2022). The river source is in the Cantabrian Mountains at 880 m.a.s.l. (extreme north–west of the basin; Fig. 1), and the river mouth is located on the Mediterranean coast in the southeastern part of the basin.

The main tributaries of the Ebro River are located on the left bank, originating from the Pyrenees, and include the Aragón-Arga (natural flow 4145 Mm^3/year) and Cinca-Segre (5423 Mm^3/year) River systems (Fig. 1), which account for 62% of the total flow of the Ebro River (data for 1980–2017; CHE, 2022). The inflows from the right bank amount to only 5% of the total flow (Batalla et al., 2004). The Ebro River flow regime is influenced accordingly by the left bank tributaries, with a contribution of snowmelt in the late spring season that represents 6% of the total water supply of the Ebro River Basin (MAGRAMA, 2008). The maximum natural flow for these pluvio–nival or nivo–pluvial tributaries occur in the late spring months or even summer months (Bejarano et al., 2010; Masachs, 1948). On the other hand, the Ebro River natural flow presents a pluvial regime influenced in the middle–lower reaches by the nivo–pluvial regime of the left bank tributaries (Masachs, 1948) and is characterized by long periods of maximum flows during winter and spring (Bejarano et al., 2010).

The mean annual flow shows a significant decreasing trend in the river tributaries, between < 1% for the Aragón-Arga River and 3% for the Cinca- Segre River (Lorenzo-Lacruz et al., 2012; 1945–2005). The flow at the last gauging station was 2747 Mm^3 /year for the Aragón-Arga River and 3724 Mm^3 /year for the Cinca-Segre River (from 1980/81–2017/18; MAGRAMA, 2021). The Ebro River shows the same behavior; the mean annual flow for the final gauging station at Tortosa was 9087 Mm^3 /year in the same period (31% lower than the historic average of 13,087 Mm^3/year (1912/13–2017/18); MAGRAMA, 2021), showing a significant decreasing trend of −2.9 m^3 /s per year (Lorenzo-González et al., 2014).

Irrigated agriculture is the main water user in the Ebro River Basin, accounting for 92.2% of the total diversions (CHE, 2022). The irrigated area has been increasing steadily in recent years and reaches almost 924,000 ha (11% of the total surface), with a current demand estimated at 8141 Mm^3 /year (CHE, 2022). The irrigated surface is particularly important in the Cinca-Segre River Basin with 371,000 ha (16% of the total basin), in the Arba River Basin with 60,000 ha (28%) and less important in the Aragón-Arga River Basins with 64,700 ha (7%) (elaborated using data from CHE, 2022). The diversions for urban (483 Mm^3/year) and industrial (208 Mm^3/year) uses are much lower (CHE, 2022).

There are some reservoirs and several weirs along the main stem used for diverting water for irrigation. The Ebro Reservoir (storage capacity of 540 Mm^3) is located in the Ebro River headwaters and is managed mainly for regulation (Fig. 1). The lower reaches of the main stem are dominated by the Mequinenza Reservoir (1534 Mm^3 for hydropower generation) upstream of the confluence of the Cinca-Segre and the smaller Ribarroja and Flix Reservoirs downstream (also for hydropower generation) (Fig. 1). Other important reservoirs are located on the Pyrenean tributaries: Yesa Reservoir with 476 Mm^3 and Itoiz Reservoir with 418 Mm^3 on the Aragón River Basin; El Grado-Mediano system on the Cinca River with 835 Mm^3 ; Canelles-Santa Ana system with 915 Mm^3 ; and Rialb Reservoir with 403 Mm^3 in the Segre River Basin. These reservoirs supply water for the large, irrigated areas on the left margin: Bardenas (78,000 ha), Alto Aragón (133,000 ha), Aragón y Cataluña Canal (96,000 ha) and Urgel (66,000 ha) (CHE, 2022).

There are two main thermal discharge sources from nuclear power plants (NPPs) (Fig. 1) along the Ebro River. The Garoña NPP, located in the upper reaches of the Ebro River, was active from March 1971 to December 2012 with an annual mean output of 3800 GWh (NUCLENOR, 2013). The Garoña NPP did not have refrigeration towers and discharged to the Sobrón Reservoir (20 Mm^3). The Ascó NPP is located in the lower reaches of the Ebro River; it has been fully active since March 1986 (with two reactors: Ascó I and Ascó II). The Ascó NPP has a mean annual output of 15,000 GWh (Coll et al., 1996; ANAV, 2012), and its refrigeration effluent is discharged directly to the Ebro River downstream of the Flix Reservoir after flowing through a refrigeration tower (built in 1995). The Ascó NPP has a 77 m^3 /s water allowance for refrigeration and another 29 m^3 /s for thermal dilution (CHE, 2008).

Finally, the main cities along the Ebro River, Zaragoza (population 680,000) and Logroño (population 154,000) and, to a lesser extent Miranda de Ebro (population 38,000) in the upper reach, and their surrounding industrial areas may be another source of thermal affection (Fig. 1). The effluents of another four cities may affect the T_w in some left bank tributaries: Lleida (population 138,000) on the Segre River, Vitoria (population 245,000) on the Zadorra River, Pamplona (population 195,000) on the Arga River, and Huesca (population 52,000) on the smaller Isuela River.

2.2. Database

The surface water quality control network (SWQ) of the Ebro River Basin was created by the CHE and started collecting monthly T_w

data in 1972–73 (MOPU, 1990). The network started with 22 monitoring stations, and today, the number of stations in the network has increased to more than 500 (CHE, 2021a).

Twenty-one SWQ stations were selected on the Ebro River and its main tributaries for this study, 14 on the Ebro River and 7 on the main tributaries. From each station, the instant monthly data of T_w, T_a (CHE, 2021a; MOPU, 1990), the flow at the time of measurement (Q_i) (CHE, 2021a; MOPU, 1990) and the mean monthly flow (Q_m) (MAGRAMA, 2021) were retrieved (one data point per month). Both T_w and T_a series were screened, and the values that were deemed blunt errors were eliminated. The sampling frequency was reduced in 2012 from monthly to quarterly, and thus, the data analyzed in this work correspond to monthly data in the 40-year period from October 1973 to September 2012, missing 8 years with a strong increase in air temperature (from 2012 to 2020). The information from 2012 to 2022 was not included to avoid spurious influences in the establishment of trends for months with missing data.

There were two important factors in the selection of the stations: long and (reasonably) complete data series and the plausibility of the stations to be affected by the main temperature drivers in the Ebro River Basin; thus, they were located downstream of nuclear power plants, regulated reaches, reservoirs, and main irrigation areas or on the main tributaries (Table 1; Fig. 1). Data series at some stations were not complete (Table 1). Thus, the period from October 1975 to September 2008 was selected to compare the behavior of T_w throughout the year at all stations, while the trends were analyzed with the longest series available at each station.

Two stations were selected in the headwaters of the Aragón (Aragón Jaca station [18])[2] and Segre Rivers (Segre Seo station [23]), presumably with little or no thermal effects, and one in the headwaters of the Ebro River (Ebro Cereceda station [161]), 125 km downstream of the Ebro Reservoir. The thermal conditions and their changes along the main tributaries were monitored with data from the Arga Peralta [4], Aragón Caparroso [5] (Aragón-Arga River system), Cinca Fraga [17], Segre Serós [25] (Cinca-Segre River system) and Arba River Tauste stations [60]. In the upper reach of the main stem, the Ebro Miranda station [1] is the first quality station downstream of the Garoña NPP, and the Ebro Haro station [208] may also be affected by Garoña NPP effluent (48 km upstream), whereas the Ebro Ascó [163], Xerta [212] and Tortosa [27] stations are located downstream of the Ascó NPP. Along the Ebro River middle reaches, the main thermal influences are diversions for irrigation: Ebro Pignatelli [162], Pina [211] and Xerta [212]. In addition, influences due to inflows from tributaries, Ebro Castejón [2]. The stations in the lower Ebro River reaches are also affected by the flow regulation of the Mequinenza Reservoir, Ebro Mequinenza station [29], with two stations located downstream of the confluence of the Cinca River on smaller reservoirs, the Ebro Flix [210] and Ebro Ascó stations [163] (Table 1).

Finally, 3 stations from the Spanish Meteorological Agency (AEMET, 2022) were selected to analyze monthly T_a trends: 9170-Logroño, 9434-Zaragoza airport and 9981A-Tortosa. These stations are the closest ones to 3 quality stations on the Ebro River used in this work (Lodosa, Zaragoza and Tortosa, respectively) and unlike the water quality stations, they have very complete data series of mean daily T_a from 1973/74–2011/12.

2.3. Statistical procedures

2.3.1. Water temperature characterization

The T_w annual cycle was characterized through a harmonic equation fitted by regression on the number of months since the beginning of the time series (N), which also allowed for the calculation of the average trend:

$$T_w = b_0 + b_1 \cdot N + c_1 \cdot \sin(N \cdot \pi/6) + d_1 \cdot cos(N \cdot \pi/6) + c_2 \cdot \sin(N \cdot \pi/3) + d_2 \cdot cos(N \cdot \pi/3) \quad (1)$$

where b_0 (intercept of the regression) is the T_w the month prior to the beginning of the series (N = 0) and b_1 is the regression coefficient for N (an estimate of the trend in °C/month). With 12 measurements per year, c_k and d_k are the regression coefficients of the transformed variables sin (k·N·π/6) and cos (k·N·π/6), which account for cycles with angular frequency $\omega = 2 \cdot \pi \cdot k/12 = k \cdot \pi/6$; that is, for cycles with a period T = 1/k yr and frequency $\nu = k\ yr^{-1}$. Other higher and lower frequencies were tried, but only the cycles with Frequencies 1 and 2 (periods of one year and six months, respectively) were significant ($P < 0.05$) in at least one of the transformed variables (sine or cosine) for all series, while no other frequency showed significant coefficients. Thus, only the harmonics of order two were fitted to all stations.

From the trigonometric identity

$$\cos(a - b) = \cos a \cdot \cos b + \sin a \cdot \sin b \quad (2)$$

Eq. (1) can be rewritten as:

$$T_w = b_0 + b_1 \cdot N + A_1 \cdot cos(N \cdot \pi/6 - \varphi_1) + A_2 \cdot cos(N \cdot \pi/3 - \varphi_2) \quad (3)$$

with

$$A_k = \sqrt{c_k^2 + d_k^2};\ \varphi_k = \arctan(c_k/d_k) k = 1, 2 \quad (4)$$

which allows for a more direct interpretation of the parameters: A_k and φ_k are the amplitude and phase angle of the wave of frequency k (yr^{-1}), respectively. The phase angle in radians may be converted to months or days with:

[2] The number indicates the station ID in the surface water quality control network (SWQ).

Table 1
Monitoring stations in the Ebro River Basin SWQ network used in this work with their T_w control factors (RG, regulated river stretch; RS, station located on reservoir; MT, downstream from the main tributaries; PP, nuclear power plants; IR, receiving irrigation return flows and WD, water diversion), distance to the source (D), altitude of the station above sea level (Z), surface of the contributing basin (S), available data series and percent of missing observations of water temperature (T_w) data from October 1975 to September 2008 (MD).

River	ID Station	Stations	RG	RS	MT	PP	IR	WD	D (km)	Z (m)	S (km^2)	Available Date Series	MD%
Ebro	161	Ebro Cereceda	+						145	547	4530	Oct-74/Jul-09	8.5
	1	Ebro Miranda	+			+			235	453	5480	Oct-73/Sep-12	1.0
	208	Ebro Haro	+			+			256	441	7300	Oct-75/Jun12	2.1
	120	Ebro Lodosa	+				+		363	319	12010	Oct-73/Sep-12	5.3
	2	Ebro Castejón			+		+		436	260	25195	Oct-73/Sep-08	4.8
	162	Ebro Pignatelli					+	+	467	249	26430	Oct-75/Sep-12	1.8
	11	Ebro Zaragoza					+		581	198	40435	Oct-73/Jul-12	0.8
	211	Ebro Pina					+		606	169	47130	Oct-74/Sep-12	1.5
	112	Ebro Sástago						+	671	138	48975	Oct-73/Jul-09	7.0
	29	Ebro Mequinenza	+	+					814	121	57440	Oct-76/Ago-12	13.1
	210	Ebro Flix	+	+	+				846	41	81060	Oct-75/Jul-12	5.9
	163	Ebro Ascó	+			+			888	25	82245	Oct-80/Sep-12	18.9
	212	Ebro Xerta	+			+			908	7	82970	Oct-76/Sep-12	34.7
	27	Ebro Tortosa	+			+		+	922	1	84230	Oct-73/Sep-12	1.0
AragónArga	18	Aragón Jaca							33	765	240	Oct-73/Ene-09	9.1
	5	Aragón Caparroso	+				+		174	300	5470	Oct-73/Sep-12	7.0
	4	Arga Peralta	+				+		143	278	2760	Jun-74/Sep-12	7.0
Cinca Segre	23	Segre Seo							67	672	560	Oct-74/Feb-12	8.2
	25	Segre Seros	+				+		255	87	12780	Oct-73/Sep-12	5.3
	17	Cinca Fraga	+				+		177	98	9610	Oct-73/Sep-12	2.6
Arba	60	Arba Tauste					+		93	243	2190	Oct-74/Sep-12	7.9

$$\varphi(month) = 6 \cdot \varphi(rad)/\pi;\ \varphi(day) = 365.25 \cdot \varphi(rad)/(2 \cdot \pi) \quad (5)$$

with a positive (negative) sign indicating the days after (before) the observation for which N = 0 or multiples of 12 when the cycle achieved its maximum.

The significance of the linear regression between estimated and measured T_w values was used to indicate the goodness of the fit.

2.3.2. Relationships between T_w and auxiliary variables

The most important parameter controlling water temperature is T_a. A good (or bad) relationship between T_a and T_w points to a small (or large) influence of other factors and little (or large) thermal inertia at that location. Therefore, in this study, we used the simple linear regression of T_w on T_a to identify the stations where T_a exerted a greater influence on T_w:

$$T_w = a + b \cdot T_a \quad (6)$$

Another parameter naturally related to T_w is the flow. Thus, we analyzed the relationship between T_w and the mean monthly flow (Q_m) at each station. We used Q_m instead of the instantaneous flow at the time of T_w measurement (Q_i) because the monthly flow series was far more complete. A logarithmic equation was selected because it showed the best fit at all stations.

$$T_w = a + b \cdot \ln(Q_m) \quad (7)$$

2.3.3. Trend analysis

Two parametric regression methods (linear regression of T_w for each individual month and harmonic analysis) and one nonparametric method (seasonal Kendall test along with the seasonal Kendall slope estimator; Gilbert, 1987) were used to detect and estimate trends in the original T_w series.

2.4. Linear regression by month

For a given month (i), the linear regression of the mean monthly temperature in that month (T_{wi}) on the year (Y, taken as 1 for the first year in each series).

$$T_{wi} = a_i + b_i \cdot Y \quad (8)$$

yields a slope (b_i) that can be regarded as the trend in T_w over time (expressed in °C yr^{-1}) for month "i". The trends in a given month "i" were considered significant when the slopes b_i were significantly different from 0 ($P < 0.05$). The intercept a_i yields the value of T_w in month "i" of year 0; that is, the year right before the beginning of the analyzed series.

2.5. Harmonic regression analysis

In the harmonic regression Eq. (3), T_w was fitted to two cosine waves plus a trend. The regression coefficient b_1 in Eq. (3) yields the increase/decrease in T_w per month (°C/month) and can be taken as the linear trend in T_w at each station. The trend of T_w at a given station was significant if the parameter b_1 was significantly different from 0 ($P < 0.05$).

2.6. Seasonal Kendall slope estimator

The nonparametric seasonal Kendall test for trend (Hirsch et al., 1982) was used to assess the presence of significant trends ($P < 0.05$), and the seasonal Kendall slope estimator (based on the Sen Median slope estimator) was used to determine the trend in each month and for the whole year (Hirsch et al., 1982). The homogeneity of the trends among months at each station was checked using a χ^2 test ($P = 0.05$) (Gilbert, 1987).

The Mann–Kendall method (Mann, 1945; Kendall, 1975) was selected because it can be used for non-complete data series and without any particular distribution (Gilbert, 1987). This method is commonly used to analyze hydrometeorological and water quality trends of variables such as flow, precipitation, salinity or temperature (Webb and Nobilis, 1995; Kaushal et al., 2010; López-Moreno et al., 2011; Prats et al., 2007; Bouza, 2006).

3. Results

The harmonic equation presented a good adjustment in the 21 stations, with a significant linear relation between estimated and observed T_w values (R^2=0.782–0.927, Table 2).

There were many missing data in the T_w series (Table 1), and in addition, T_w observations, although with monthly frequency, were taken randomly in day and hour within each month. The harmonic equation fills T_w monthly gaps and decreases the effects due to measurements in a non-representative day/hour. Therefore, the values estimated by the harmonic equation were used to calculate annual and monthly T_w averages, the months of maximum and minimum T_w and the range (difference between the maximum and minimum monthly T_w) at the different stations (Table 2).

Table 2
Mean annual water temperature (T_w) and annual temperature range (R) and results from the first- and second-order harmonics fitted to the T_w data for the 21 stations selected: amplitude (A_1 and A_2) and phase angle (φ_1 and φ_2, days from October 1, first day of the hydrological year); maximum and minimum T_w and month of occurrence (mon); Mean annual water temperature (T_w-H) and annual range (R-H) estimated with the fitted harmonic model; coefficient of determination of the linear regression between estimated and observed T_w values (R^2) and standard error of harmonic equation estimates (SE). Series from October 1975 to September 2008.

	Harmonics											
	T_w-H	R-H	1st order		2nd order		Max		Min			
Stations	Mean (°C)	Range (°C)	A_1 (°C)	φ_1 (d)	A_2 (°C)	φ_2 (d)	T_w (°C)	mon	T_w (°C)	mon	R^2	SE (ºC)
Ebro Cereceda	12.7	14.0	6.8	-59	0.5	-49	20.3	Aug	6.2	Jan	0.871	1.87
Ebro Miranda	15.5	14.3	7.1	-51	0.4	-48	23.3	Aug	9.0	Jan	0.857	2.07
Ebro Haro	14.9	14.5	7.1	-52	0.5	-48	22.9	Aug	8.4	Jan	0.869	2.00
Ebro Lodosa	14.3	15.4	7.5	-57	0.6	-44	22.6	Aug	7.2	Jan	0.888	1.91
Ebro Castejón	14.0	15.1	7.4	-61	0.5	-49	22.0	Aug	6.9	Jan	0.881	1.95
Ebro Pignatelli	14.5	15.8	7.8	-59	0.4	-38	22.7	Aug	6.9	Jan	0.872	2.14
Ebro Zaragoza	14.7	16.1	7.9	-61	0.4	-34	23.0	Aug	6.9	Jan	0.873	2.17
Ebro Pina	15.2	16.3	8.1	-67	0.4	-51	23.5	Aug	7.3	Jan	0.879	2.15
Ebro Sástago	15.9	18.0	8.9	-68	0.5	-52	25.1	Aug	7.2	Jan	0.876	2.43
Ebro Mequinenza	15.9	15.0	7.5	-48	0.4	37	23.1	Aug	8.1	Feb	0.832	2.41
Ebro Flix	15.2	14.8	7.4	-50	0.5	19	22.5	Aug	7.7	Jan	0.927	1.48
Ebro Ascó	17.1	16.4	8.2	-51	0.4	6	25.4	Aug	9.0	Jan	0.907	1.90
Ebro Xerta	17.0	15.8	7.9	-54	0.4	11	24.8	Aug	9.0	Jan	0.898	1.90
Ebro Tortosa	17.3	15.7	7.8	-56	0.4	6	25.1	Aug	9.3	Jan	0.897	1.89
Aragón Jaca	9.5	12.2	5.7	-56	0.8	-62	16.8	Aug	4.6	Jan	0.782	2.24
Aragón Caparroso	13.4	15.9	8.0	-63	0.5	-72	22.0	Aug	6.1	Jan	0.862	2.36
Arga Peralta	13.5	14.4	7.2	-62	0.4	-68	21.2	Aug	6.9	Jan	0.856	2.10
Segre Seo	11.1	15.8	7.4	-68	0.9	-51	19.6	Aug	3.9	Jan	0.851	2.25
Segre Serós	14.8	15.9	7.8	-66	0.5	-33	22.8	Aug	6.9	Jan	0.885	2.01
Cinca Fraga	14.6	15.6	7.8	-69	0.4	-44	22.4	Aug	6.8	Jan	0.862	2.25
Arba Tauste	13.6	13.5	6.6	-65	0.4	-32	20.0	Aug	6.9	Jan	0.843	2.06

3.1. Water temperature patterns in the Ebro River Basin

3.1.1. Ebro River longitudinal analysis: annual and seasonal results

3.1.1.1. T_w along the Ebro River axis. Along the Ebro River main stem, the mean annual T_w (1975–2008) increased by 4.6 °C from the first upstream station at the Ebro Cereceda station to the last station at Ebro Tortosa, resulting in an average gradient of 0.6 °C/100 km. However, this increase was not homogeneous along the river (Fig. 2; Table 2):

(i) In the upper reaches, T_w increased 2.8 °C between the Ebro Cereceda (upstream of the Garoña NPP) and Ebro Miranda (downstream of the NPP) stations, separated by 90 km; an average increase of 3.1 °C/100 km.

(ii) Flowing into the Ebro Depression, T_w decreased by 1.5 °C along the 201 km stretch between the Ebro Miranda and Ebro Castejón stations, with an average variation of −0.7 °C/ km and a decrease in T_w opposite to the natural river behavior (increasing T_w downstream). The contribution of the large tributaries from the left bank (Aragón and Arga; with a flow higher than the Ebro River in this stretch, and with a lower T_w: 13.4 °C for the Aragón Caparroso station and 13.5 °C for the Arga Peralta station) could explain the decrease in T_w in the Ebro River from 14.3 °C at Lodosa to 14.0 °C at Castejón.

(iii) In the lower–middle reaches of the Ebro Depression, the Ebro River temperature rose at a rate of 0.5 °C/100 km from Castejón to Mequinenza. From the Mequinenza Reservoir (T_w = 15.9 °C) to the Flix Dam (T_w = 15.2 °C), T_w decreased by 0.7 °C, due to the discharge from the Cinca-Segre system, with lower mean T_w (14.6 °C for the Cinca Fraga station and 14.8 °C for the Segre Serós station).

(iv) Finally, in the lower reaches, downstream of the Ascó NPP, the T_w increased 1.9 °C between the Ebro Flix (15.2 °C) and Ebro Ascó (17.1 °C) stations (4.5 °C/100 km) and remained high (T_w > 17 °C) to the river mouth (Ebro Tortosa station).

3.1.1.2. Annual range of T_w along the Ebro River axis. The temperature range (difference between the maximum and the minimum mean monthly T_w) increased steadily from the Ebro Cereceda (14.3 °C) station to the Ebro Pina (16.3 °C) station at a rate of 0.5 °C/100 km (Fig. 2). Downstream of the Ebro Pina station, this range increased at a rate of 2.6 °C/100 km and had the highest T_w range at the Ebro Sástago station, which is the last station in the Ebro Depression upstream of the Mequinenza Reservoir. The Ebro Sástago station is located in the most continental and driest area of the Ebro River Basin, downstream of a reach with low slope and water speed. This increase in the annual T_w range down the Ebro River was caused mainly by the rise of summer T_w from Lodosa to Sástago (Fig. 3a). The Ebro Sástago station and the next station, Ebro Mequinenza, (not affected by NPPs stations) had the highest T_w of all stations analyzed (Fig. 2) (15.9 °C). This effect can be attributed to the natural climatic variability which is more accused in the central reaches of the Basin, with a more continental climate. However, the increase in the annual T_w range along the Ebro River Depression was reversed downstream of the Mequinenza–Ribarroja–Flix Reservoirs (Fig. 2), as reservoirs smooth river T_w (Webb, 1988). Downstream of the Mequinenza Reservoir, T_w decreased in summer and increased in winter. The maximum monthly T_w at Sástago (August) was 2.0 °C higher than that at Mequinenza, and the minimum T_w (January) was 1.2 °C lower than that at Mequinenza (Fig. 3b). From September to January, the Ebro Sástago station had a lower T_w than the Ebro Mequinenza station, and the opposite was observed from February to August (Fig. 3b).

Mixing in the Mequinenza Reservoir reduced the annual T_w range to 15.0 °C. The T_w range remained low at the Flix station (14.8 °C) after the incorporation of the Cinca-Segre flows but rose at the Ascó station to 16.4 °C only to descend downstream to 15.8 °C at the Xerta station and 15.7 °C at the river mouth at the Tortosa station (Table 2; Fig. 2). Generally, the maximum T_w was found in August, and the minimum T_w was found in January. Only in the Mequinenza Reservoir did the T_w minimum shift to February (Table 2).

The reservoirs not only affected the range of the annual T_w cycle but also shifted the month in which maximum and minimum T_w occurred in the year. At the Ebro Mequinenza station, the minimum T_w was found in February, whereas from Zaragoza to Sástago, the

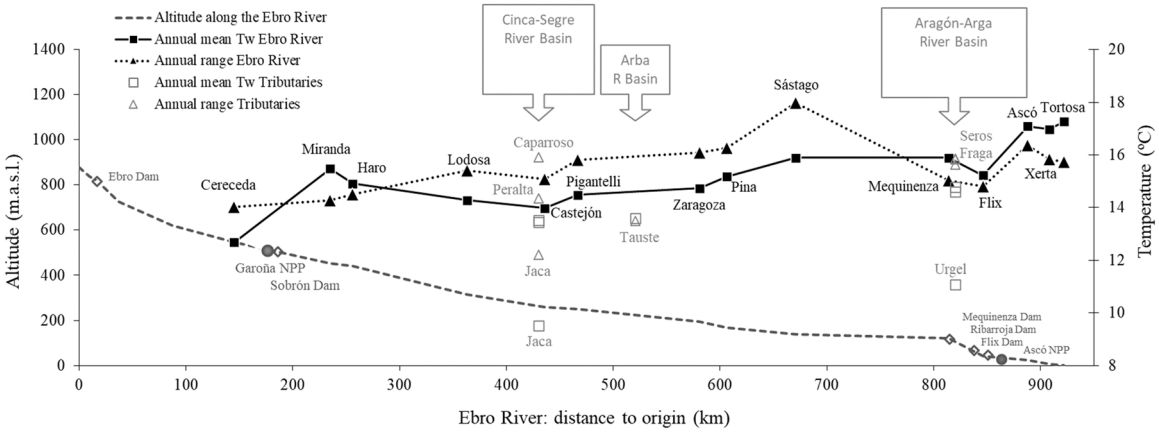

Fig. 2. Longitudinal profile of the annual mean T_w and annual range of the monthly water temperature along the Ebro River and main tributaries. For the tributaries, the graph shows the annual mean and range of T_w, at each station.

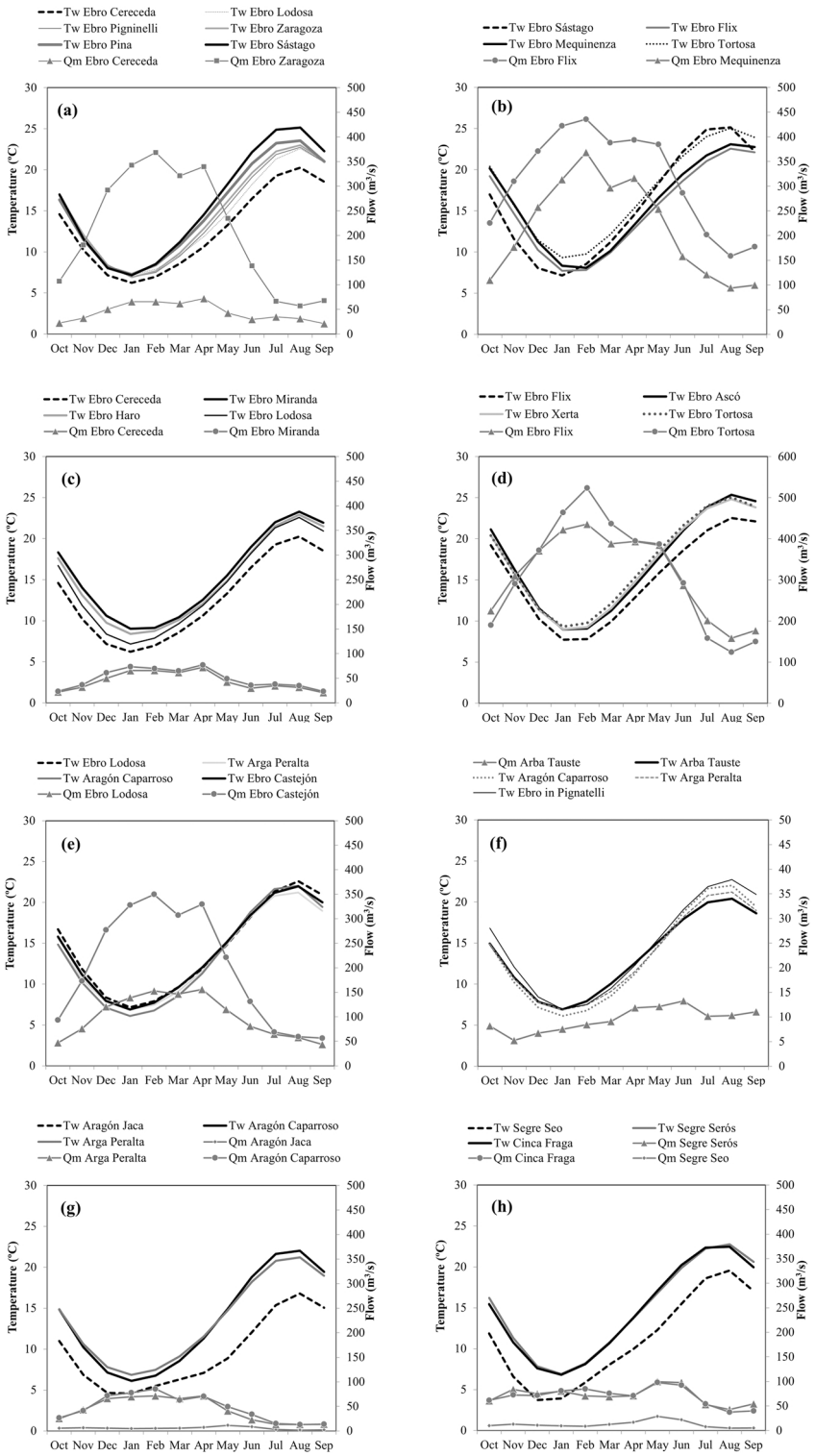

Fig. 3. Monthly T_w estimated with harmonic equations and monthly flow at the different stations on the Ebro River and main tributaries (Series October 75-September 08).

minimum occurred in January, approximately one month before. This behavior can also be appreciated through the φ_1 value (shift of the annual wave) in the harmonic equation (Table 2). At the stations downstream of the reservoirs (Ebro Mequinenza and Ebro Flix stations), φ_1 had the lowest absolute value in the basin, indicating that the maximum of the annual cycle was displaced only 48

(Mequinenza) and 50 (Flix) days before October 1, while it was moved 68 days before that date at the Ebro Sástago station (Table 2).

Throughout the basin, the peak of the annual T_w cycle occurred 51–69 days before October 1, and this shift (φ_1) was highest in the tributaries (except for the Aragón Jaca station) and in the Ebro Depression (Table 2). Along the Ebro River, this shift was higher than 56 days for all stations except for the Ebro Miranda and Haro stations (both downstream of the Ebro Reservoir) and in the stations downstream of Mequinenza, showing the impact of reservoirs in reducing this shift. In the central Ebro Depression, the shift increased downstream from 57 days at Lodosa to 68 days at Sástago.

The peak of the 6-month cycles occurred before October 1 at all stations in the basin ($\varphi_2 < 0$; Table 2), except in those downstream of the Mequinenza Reservoir, where it occurred after that date ($\varphi_2 > 0$; Table 2). Generally, the 6-month wave peaks did not follow a particular increasing or decreasing trend along the Ebro River or its tributaries (Table 2). The maximum of the 6-month wave was found just 33 days after October 1 at the mouth of the Segre (Segre Serós station) and 32 days before October 1 at the mouth of the Arba (Arba Tauste station) but 72 days before that date at the mouth of the Aragón (Aragón Caparroso station) (Table 2). Along the Ebro River upstream of Mequinenza, the maximum occurred between 6 and 52 days before October 1, with the shift being greatest at the Ebro Sástago station (Table 2).

The stations located upstream and downstream of the two NPPs showed different T_w behaviors. The stations located upstream (Ebro Cereceda station) and downstream (Ebro Miranda station) of the Garoña NPP had similar annual ranges and cycles, but the mean monthly T_w at the Miranda station was approximately 2–4 °C higher than that at the Cereceda station (Fig. 3c). On the other hand, the stations upstream (Ebro Flix station) and downstream (Ebro Ascó station) of the Ascó NPP had different seasonal behaviors. The annual range increased from the Ebro Mequinenza and Flix stations to the Ebro Ascó station at 1.9 °C (Fig. 2) (same increase that showed the average T_w; Table 2). The increase in the monthly T_w from the Flix to Ascó stations was low and constant from November to April (1.4 °C) and higher between June and September (2.4–2.8 °C) (Fig. 3d).

The Garoña NPP effluent, without a refrigeration tower, discharged into the Sobrón Reservoir. The water storage at this reservoir led to the absorption of this heat input in a similar way throughout the year (minimum monthly water storage: 16.0 Mm^3 and maximum monthly water storage: 19.7 Mm^3, from February 1997 to the closure of the Garoña NPP in 2012), with some differences due to differences in the Ebro River input-output flow into the Sobrón Reservoir; the period with low Ebro River flow and less water input into the reservoir (August to December) corresponded with the higher differences in T_w between the Cereceda and Miranda stations (>3 °C), with a peak occurring in November (3.8 °C).

3.1.2. *Tributaries: annual and seasonal results*

In the tributaries, the mean T_w and annual range increased from the headwaters to the river mouth (Table 2). The annual mean T_w increased at a rate of 2.8 °C/100 km along the Aragón River from the Jaca to Caparroso stations and 2.0 °C/100 km along the Segre

Table 3
Estimated parameters (a intercept, b slope) of the linear regression equations established between the measured monthly water temperature (T_w) and the air temperature at the time of sampling (T_a) and the natural logarithms of the mean monthly flow (Q_m): coefficients of determination (R^2) and standard error of the estimates (SE). Level of significance: *** $P < 0.001$; ** $P < 0.01$; and * $P < 0.05$. The mean monthly water temperature (T_w), mean monthly air temperature (T_a) in the station, and mean monthly flow (Q_m) are also given (all available data for the period 1973/74–2011/12).

	$T_w - T_a$				$T_w - Q_m$						
	$T_w = a + b \cdot T_a$				$T_w = a + b \cdot \ln(Q_m)$				Annual average		
Stations	a	b	R^2	SE	a	b	R^2	SE	T_w (°C)	T_a (°C)	Q_m (m^3/s)
Ebro Cereceda[(2)]	4.172	0.601	0.762***	2.55	19.16	-1.90	0.078***	5.06	12.6	14.1	44
Ebro Miranda	6.124	0.626	0.668***	3.22	28.35	-3.60	0.202***	4.99	15.5	15.0	49
Ebro Haro[(1)]	4.610	0.703	0.719***	2.93	24.73	-2.62	0.172***	5.01	15.0	14.6	–
Ebro Lodosa	2.957	0.750	0.782***	2.68	33.41	-4.38	0.266***	4.92	14.4	15.2	99
Ebro Castejón	4.817	0.587	0.545***	3.80	35.03	-4.29	0.484***	4.07	14.0	15.5	197
Ebro Pignatelli[(2)]	2.747	0.741	0.812***	2.63	33.12	-3.96	0.544***	4.03	14.6	16.0	225
Ebro Zaragoza	3.078	0.709	0.815***	2.62	35.03	-4.29	0.484***	4.07	14.9	16.5	207
Ebro Pina[(1)]	3.722	0.657	0.817***	2.67	38.45	-4.16	0.550***	3.81	15.2	17.4	–
Ebro Sástago[(2)]	3.105	0.733	0.795***	3.12	42.41	-5.35	0.480***	4.90	15.8	17.3	222
Ebro Mequinenza	6.235	0.550	0.618***	3.65	35.02	-3.82	0.276***	4.98	15.9	17.5	212
Ebro Flix	4.363	0.581	0.709***	2.98	40.11	-4.47	0.230***	4.82	15.3	18.8	312
Ebro Ascó[(2)]	4.154	0.655	0.725***	3.25	47.01	-5.30	0.245***	5.30	17.2	20.0	303
Ebro Xerta[(1)]	3.345	0.671	0.709***	3.21	30.05	-2.39	0.134**	5.44	17.1	20.5	–
Ebro Tortosa	2.293	0.729	0.771***	2.86	45.80	-5.20	0.366***	4.74	17.3	20.6	312
Aragón Jaca	1.793	0.516	0.724***	2.50	11.45	-1.46	0.086***	4.57	9.5	14.9	5
Aragón Caparroso	2.031	0.747	0.827***	2.55	24.20	-3.19	0.296***	5.12	13.5	15.3	45
Arga Peralta	2.415	0.740	0.828***	2.32	26.86	-3.92	0.444***	4.15	13.6	15.1	44
Segre Seo	1.169	0.593	0.771***	2.78	13.79	-1.25	0.034**	5.72	11.0	16.5	12
Segre Seros	3.330	0.697	0.839***	2.35	22.54	-1.90	0.039***	5.76	14.8	16.3	69
Cinca Fraga[(2)]	2.641	0.708	0.858***	2.29	23.29	-2.13	0.056***	5.65	14.6	16.9	69
Arba Tauste	3.848	0.615	0.798***	2.35	10.43	+ 1.64	0.041***	5.17	13.6	16.0	7

[(1)] Stations with no Q_m data available; the instantaneous flow data Q_i were used.
[(2)] Stations with incomplete flow data.

River from the Seo to Serós stations. The Arga River flows into the Aragón at Peralta (Arga Peralta station), very close to the mouth of the Aragón into the Ebro, with a T_w (13.5 °C) very similar to that of the Aragón at its mouth (13.4 °C, Aragón Caparroso station). In the same way, the Segre River joins the Cinca a few kilometers downstream of the Segre Serós station, very close to the Cinca Fraga station. The T_w at the Segre Serós station (14.8 °C) and Cinca Fraga station (14.6 °C) were also very similar (Table 2).

The stations located at the river mouth of the main tributaries had similar annual T_w ranges to those located in the middle reaches of the Ebro River (Pignatelli to Pina stations), (~16 °C) with the exception of the Arga Peralta station (Table 2). This station had higher T_w in autumn and winter and lower T_w in summer than the Aragón Caparroso station (Fig. 3g).

Another seasonal T_w feature in the tributaries relative to the natural climate variability could be found at the headwater stations (Segre Seo and Aragón Jaca stations), where the higher flows occurred in May and June (Figs. 3g and 3h) due to snowmelt. At these stations, the amplitude of the six-month wave (φ_2) was much higher (A_2=0.8 °C at Jaca and 0.9 °C at Seo) than at the rest of the stations in the basin (A_2 from 0.4 °C to 0.6 °C) (Table 2), pointing to a greater influence of snowmelt. This fact was also shown by the evolution of T_w throughout the year at both stations, with a clear decrease from the annual cycle in spring (Figs. 3g and 3h).

The effects of the Aragón-Arga, Arba and Cinca-Segre tributary systems on the Ebro River T_w were different. The Aragón River flows into the Ebro River downstream of the Ebro Lodosa station and upstream of the Ebro Castejón station. The tributary mouth stations (Arga Peralta and Aragón Caparroso stations) had lower T_w than the Ebro Lodosa station in all months except for spring, and it was only in this season that T_w increased slightly (<0.3 °C) from Lodosa to Castejón (Fig. 3e). For the rest of the year, T_w was higher at Lodosa than at Castejón, with the maximum difference found in September-October (0.9 °C).

The Arba River mouth station at Tauste had an annual range of only 13.5 °C, the lowest annual range only after the Aragón Jaca station (Table 2) and quite unlike the other tributaries on the left margin (Aragón-Arga and Cinca-Segre) (Fig. 2).

On the other hand, the Cinca-Segre system discharges to the Ebro River into the Ribarroja Reservoir, downstream of the Mequinenza Reservoir. The effect of the Cinca-Segre discharge on the Ebro River T_w supersedes the effect of the Mequinenza Reservoir (largest reservoir in the basin, 1500 Mm^3) with a marked influence on the annual T_w cycle.

3.2. *Relationship of T_w – T_a and T_w – streamflow*

All stations analyzed showed a high correlation between air temperature and water temperature (T_a and T_w taken simultaneously), but some differences were found between stations. The linear relationship between T_a and T_w (Table 3) was strong (R^2>0.80; SE<3.12 °C) in the Ebro Depression from Pignatelli to Sástago and at the tributary mouths (Arga Peralta, Aragón Caparroso, Cinca Fraga, Segre Serós, and Arba Tauste stations). These stations are characterized by a common physical river morphology with open valleys, meandering reaches and low water velocity, while their main effects come from irrigated, industrial and urban areas.

The relationship was weaker (R^2=0.70–0.80; SE=2.86–3.65 °C) at the stations downstream of the reservoirs (Ebro Flix station) and the NPPs (Ebro Haro, Ebro Ascó, Ebro Xerta and Ebro Tortosa stations), where the different thermal effects had a higher weight on T_w than on T_a.

The stations located in the headwaters, Aragón Jaca and Segre Seo stations, also had a weaker relationship between T_w and T_a (R^2 =0.70–0.80; SE= 2.50–2.78 °C). In this case, the effect of snowmelt in spring, the different behavior of water and air at freezing temperatures in winter or even the high-speed flow and changes in the T_a with altitude could weaken this relationship.

The relationship between T_w and T_a was even weaker (R^2<0.70; SE>3.22 °C) at the Ebro Miranda, Ebro Castejón and Ebro Mequinenza stations. At the Miranda station, the T_w was largely controlled by Garoña NPP discharges and the absorption of this heat input by Sobrón Reservoir, as shown by its seasonal behavior. At the Mequinenza station, the heat storage in the reservoir and the altered regime of seasonal inputs- and outputs- controlled T_w in addition to T_a, while at the Castejón station, T_w was also affected by discharges from the Aragón-Arga system.

In general, the relationship between T_w and flow in the Ebro River and main tributaries, although statistically significant, was weaker than that with T_a. At all stations except for the Arba Tauste station, T_w decreased with Q_m (higher flows caused lower T_w). The coefficient of determination at most study stations was lower than 0.50, and the standard error (SE) was higher than 4 °C (Table 3).

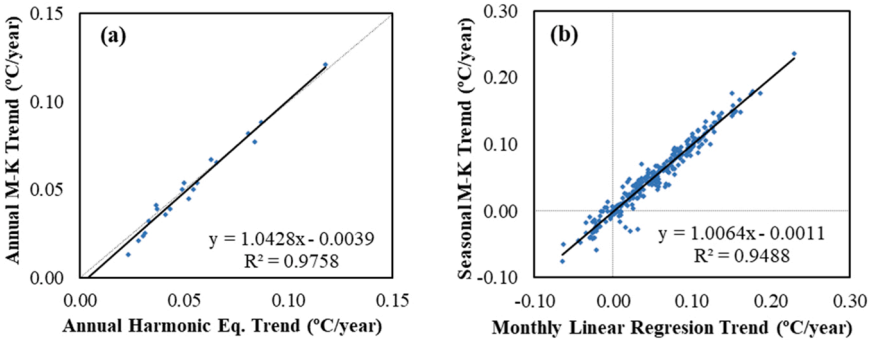

Fig. 4. Linear regression between annual T_w trends calculated by the seasonal Kendall method and by the harmonic equation method (a) and the monthly T_w trends calculated by the seasonal Kendall method and by the monthly linear regression method (b).

The relationship between T_w and flow was stronger at the stations located throughout the Ebro River Depression from Castejón to Sástago (R^2>0.45; SE<4.10 °C). The Ebro River stations downstream of the main reservoir and NPP discharges, from Miranda to Haro and from Mequinenza to Xerta, had weaker relationships (R^2<0.30; SE> 4.74 °C).

The tributaries with greater irrigation development in their basins (Cinca Fraga and Arba Tauste stations) had the weakest relationships at the stations at the river mouths (R^2<0.10; SE>5.1 °C); for the Arba River, the relationship was also inverted (b>0) in relation to the other stations. At this station, higher flows corresponded with higher T_w during the summer months.

Finally, the stations in the headwaters (Segre Seo, Aragón Jaca and Ebro Cereceda stations) also had very weak relationships (R^2<0.10; SE>4.6 °C).

3.3. Trends in water temperature in the Ebro River Basin

The annual trend estimates using the harmonic equation and the Mann–Kendall method (M–K) were similar, with a very strong linear relationship and coefficient of determination, R^2= 0.976 (Fig. 4a). The monthly trends obtained by linear regression for each month and by the seasonal Kendall slope estimator also showed a very strong linear relationship (R^2 = 0.949) (Fig. 4b). In both cases, the slopes of the linear regressions were not significantly different from 1, and the intercepts were not significantly different from 0 (P > 0.95), indicating nonsignificant differences in the trends estimated by the different methods (Fig. 4; Table 4).

The seasonal Kendall slope estimator was chosen to evaluate the T_w trends because this method (i) does not require normal data, (ii) is less sensitive to outliers, and (iii) allows for testing the homogeneity of trends in different seasons and identifying months with higher trends.

Table 4
Monthly and annual T_w trend (°C/year) estimated by the seasonal Kendall slope estimator method. The stations with a significantly homogeneous trend for all months are marked with H-U, and the stations with a homogeneous trend not significantly different from 0 in all seasons are marked with H-0. Significant trends are shadowed (p<0.05).

ΔTw (°C/year)	Oct	Nov	Dec	Jan	Feb	Mar	Apr	May	Jun	Jul	Aug	Sep	Year
Ebro River													
Cereceda	0.032	0.046	0.056	0.009	0.038	-0.016	**0.111**	**0.090**	**0.094**	0.010	0.059	-0.047	**0.039**
Miranda	0.029	0.036	0.024	**0.075**	0.000	0.040	**0.061**	**0.147**	**0.133**	0.068	-0.025	0.008	**0.054**
Haro	0.019	0.011	0.000	**0.067**	0.000	0.000	**0.124**	**0.096**	**0.148**	**0.079**	0.036	0.020	**0.050**
Lodosa	-0.038	0.026	0.016	0.030	0.006	-0.031	**0.108**	**0.112**	0.083	0.067	-0.002	-0.014	**0.025**
Castejón H-U	-0.002	0.025	0.036	0.042	0.058	0.043	0.074	**0.091**	**0.177**	0.057	0.011	-0.017	**0.045**
Pignatelli H-U	0.036	0.042	0.042	**0.090**	0.038	0.000	**0.150**	**0.127**	**0.146**	**0.083**	0.055	0.000	**0.065**
Zaragoza H-U	0.058	0.043	0.033	0.050	0.008	0.022	**0.085**	**0.125**	**0.109**	0.068	0.050	0.043	**0.054**
Pina	0.006	-0.012	0.004	0.056	-0.010	**0.085**	0.064	**0.137**	**0.107**	0.078	0.006	-0.008	**0.039**
Sástago H-U	0.030	0.019	**0.085**	**0.060**	0.030	**0.106**	0.032	**0.177**	**0.236**	**0.120**	0.063	0.048	**0.077**
Mequinenza H-U	-0.050	0.000	0.048	0.043	**0.064**	0.055	0.071	**0.100**	0.039	0.039	0.070	-0.041	**0.036**
Flix	-0.021	-0.031	0.030	0.038	0.043	0.040	**0.058**	**0.058**	**0.089**	**0.074**	**0.050**	0.036	**0.041**
Ascó H-U	0.048	0.035	0.063	**0.147**	**0.142**	**0.140**	**0.143**	**0.175**	**0.179**	**0.167**	**0.107**	**0.121**	**0.121**
Xerta H-U	0.043	0.049	**0.074**	**0.089**	**0.074**	0.037	0.085	**0.150**	**0.135**	**0.100**	0.040	**0.089**	**0.082**
Tortosa H-U	0.059	0.019	**0.084**	**0.097**	**0.067**	**0.092**	**0.100**	**0.095**	**0.159**	**0.133**	**0.083**	0.048	**0.088**
Aragón-Arga River Basin													
Aragón Jaca H-0	**0.116**	0.025	0.011	0.008	0.014	**0.043**	-0.026	-0.030	-0.058	0.042	-0.007	-0.027	0.013
Aragón Caparroso	**0.104**	0.050	-0.007	-0.023	-0.005	-0.042	0.070	**0.100**	**0.094**	-0.018	0.046	-0.033	0.021
Arga Peralta H-U	0.061	0.058	0.000	0.022	0.013	-0.040	**0.096**	**0.105**	**0.079**	-0.044	-0.006	0.000	**0.023**
Cinca-Segre River Basin													
Segre Seo H-0	0.003	0.005	0.000	-0.017	-0.018	0.000	-0.030	0.029	**0.120**	-0.033	0.052	-0.075	0.000
Segre Serós H-U	**0.096**	0.036	-0.013	0.042	-0.025	0.062	0.050	0.000	0.048	0.044	0.004	0.039	**0.032**
Cinca Fraga	0.028	0.031	-0.008	0.065	0.007	**0.091**	**0.105**	0.022	0.100	**0.125**	**0.118**	**0.088**	**0.067**
Arba River Basin													
Arba Tauste H-U	**0.115**	**0.064**	0.025	0.022	0.038	0.012	**0.057**	**0.095**	0.091	0.008	0.050	0.019	**0.050**

0.000	Significant trend (p<0.05)
0.000	Non-Significant trend

3.3.1. Annual trends

The annual trend increased downstream on the Ebro River from 0.04 °C/year at Cereceda to 0.09 °C/year at Tortosa, showing some irregularity along the river (Fig. 5). In the upper reaches, the rate of T_w increase (ΔT_w) rose from 0.04 °C/year at Cereceda to 0.05 °C/year at Miranda and Haro and then declined to 0.03 °C/year at the next station, Lodosa. Along the Ebro Depression, ΔT_w remained between 0.04 and 0.06 °C/year, reaching the highest value at Sástago, $\Delta T_w = 0.08$ °C/year.

In the stations located in the Mequinenza and Flix reservoirs, ΔT_w was lower than that at the upstream stations, approximately 0.03–0.04 °C/year, and finally, ΔT_w showed a large increase at the last stations, from Ascó ($\Delta T_w = 0.12$ °C/year), where it reached the highest value in the basin, to Xerta ($\Delta T_w = 0.08$ °C/year) and Tortosa ($\Delta T_w = 0.09$ °C/year).

The thermal discharges from the NPPs increased the annual ΔT_w at the stations located immediately downstream. The two stations immediately downstream of the Garoña NPP, Ebro Miranda and Ebro Haro stations, had higher annual trends (0.05 °C/year) than those upstream of the Ebro Cereceda station (0.04 °C/year) and downstream of the Ebro Lodosa station (0.03 °C/year) (Table 4).

In the case of the Ascó NPP, this effect was higher; ΔT_w was 0.04 °C/year at Flix, upstream of the NPP, but 0.12 °C/year at Ascó, downstream. The mean annual ΔT_w of all stations on the Ebro River was close to 0.05 °C/year (1.9 °C increase from 1973 to 2012), while at the Ebro Ascó station, it reached 0.12 °C/year (equivalent to an increase of 4.5 °C from 1973 to 2012).

The annual trend in the middle Ebro River at Sástago reached 0.08 °C/year and decreased at the stations downstream of the reservoirs (Ebro Mequinenza and Ebro Flix stations) to 0.04 °C/year. Water storage in the reservoirs may have contributed to reducing the ΔT_w, but although lower, ΔT_w remained significant at these two stations.

The annual T_w increased significantly at all tributary river mouth stations (except the Aragón Caparroso station), ranging from 0.03 °C/year in the Arga and Segre Rivers to 0.05 °C/year in the Arba and 0.07 °C/year in the Cinca (Table 4).

A general annual trend in average Q_m and T_a was observed in all the stations in the Ebro River that could be responsible for the observed trend in T_w. At the main Ebro River stations with more completed data series (Ebro Lodosa, Zaragoza and Tortosa,) mean annual flow presented a significant trend that was estimated from − 2.23 to − 7.45 Mm^3 /year (Table 5, Fig. 6). Average annual T_a trends in Ebro at Logroño, Zaragoza and Tortosa (AEMET, 2022) were significant ($P < 0.05$) and were quantified in 0.033, 0.050 and 0.040 °C/year respectively (Table 5). The trend in T_a was close to the trend in T_w in Logroño and Zaragoza (0.025 and 0.054ºC/year respectively) but was only half of the T_w trend in Tortosa (0.088 °C/year) (Table 4).

3.3.2. Seasonal trends in T_w

The trends in the headwaters of the Ebro River, from Cereceda to Lodosa, were not homogeneous between months. However, monthly trends were homogeneous, with an upward trend at all stations along the Ebro River downstream of Castejón except at the Ebro Pina and Flix stations (Table 4). The trends in the headwater stations of the Pyrenean tributaries (Aragón Jaca and Segre Seo stations) were homogeneous in all months and no-significantly different from zero, indicating that there was no global upward trend at the upper Pyrenees stations (Table 4). At the downstream end of the tributaries, there was a monthly homogeneous upward trend at the Arga Peralta, Segre Serós and Arba Tauste stations but not at the Aragón Caparroso and Cinca Fraga stations (Table 4).

The T_w trends at all Ebro River stations increased from autumn to spring, except for February and March, when some stations had lower trends (Table 4) and had significant upward trends from April to July, being significant in May in all of them (Table 4).

At the stations downstream of the Ebro Ascó station, there were also many months with significant T_w trends from December to March and in August-September. Among the tributary mouth stations, only the Arga Peralta, Aragón Caparroso, and Arba Tauste stations followed the pattern observed in the Ebro River downstream of Castejón, while the Segre Serós station only had significant trends in October and the Cinca Fraga station only in March, April and July to September (Table 4). At the Pyrenean headwater stations, there were only two singular months with significant trends: October at the Aragón Jaca station and June at the Segre Seo station (Table 4).

Aggregating the monthly data into seasons, the spring (April to June) average trend was higher than 0.08 °C/year for all stations on the Ebro River except for those in the lower reach reservoirs (Mequinenza and Flix) (Fig. 7). In all stations except the Ebro Mequinenza

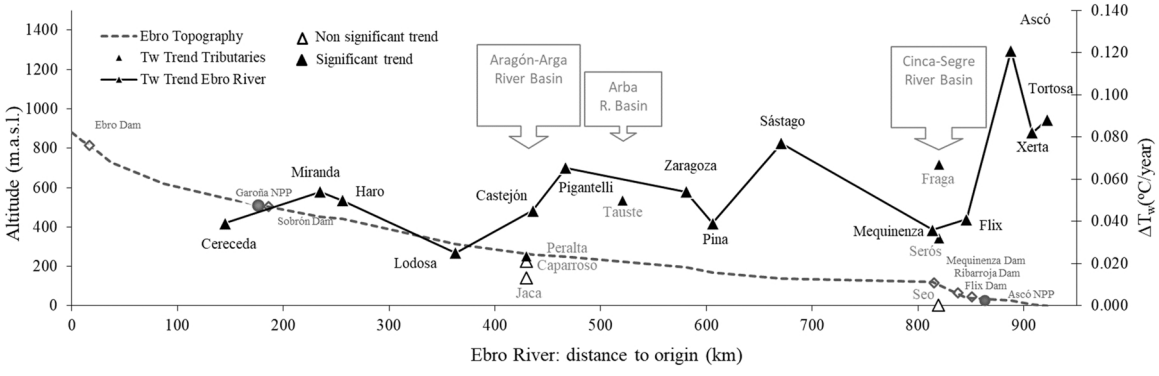

Fig. 5. Profile of the annual trends in water temperature (ΔT_w; °C/year) along the Ebro River and main tributaries obtained by the Mann–Kendall method (M-K). For the tributaries, the graph shows the annual trend at each station.

Table 5
Mean monthly (Q, Mm^3/month) and annual flow (Q, Mm^3/year) for the main Ebro River gauging stations and their trends (ΔQ, Mm^3/year), mean monthly water temperature (T_w, °C) at the corresponding quality stations, and mean monthly and annual air temperature (T_a, °C) at the meteorological stations closer to the Ebro River main stations and their trends (ΔT_a, °C/year). Series from 1973/74–2011/12. Significant trends are shadowed ($p<0.05$).

Flow (Q, Mm^3/month) and flow trend (ΔQ, Mm^3/year)

		Oct	Nov	Dec	Jan	Feb	Mar	Apr	May	Jun	Jul	Aug	Sep	Year
Ebro Lodosa	Q	127	204	323	366	374	394	401	298	207	169	150	111	3.124
	ΔQ	**-2.55**	-1.13	-0.66	-2.71	-2.75	-1.28	**-8.87**	-3.64	**-1.41**	**-1.77**	**-1.90**	**-2.28**	**-2.23**
Ebro Zaragoza	Q	285	482	757	883	901	868	861	611	347	172	148	175	6489
	ΔQ	**-4.00**	-0.98	-5.27	-6.53	-10.40	-6.55	**-17.77**	-8.63	**-2.91**	**-2.06**	**-1.56**	-0.91	**-3.16**
Ebro Tortosa	Q	508	735	961	1178	1247	1181	1051	1008	769	442	339	396	9817
	ΔQ	**-7.81**	**-12.26**	-8.94	-8.51	-17.81	-8.80	**-14.91**	-10.41	**-13.19**	**-6.14**	0.59	**-4.71**	**-7.45**

T_w (°C), T_a (°C) and T_a trend (ΔT_a, °C/year)

		Oct	Nov	Dec	Jan	Feb	Mar	Apr	May	Jun	Jul	Aug	Sep	Year
Ebro R. Lodosa	T_w	16.6	11.6	8.5	7.1	8.2	9.9	11.8	14.8	18.6	21.8	22.6	20.7	14.4
9170-Logroño	T_a	14.4	9.4	6.5	6.0	7.4	10.1	11.9	15.7	19.9	22.5	22.6	19.3	13.8
	ΔT_a	**0.053**	0.020	-0.008	0.003	-0.013	0.028	**0.067**	**0.076**	**0.086**	0.033	**0.050**	0.021	**0.033**
Ebro R. Zaragoza	T_w	17.0	12.1	8.1	6.8	8.0	10.2	13.3	16.5	19.8	22.7	23.1	20.7	14.9
9434-Zaragoza	T_a	15.9	10.3	7.0	6.5	8.3	11.3	13.5	17.7	22.2	24.9	24.8	21.0	15.3
	ΔT_a	**0.062**	0.040	-0.004	0.009	-0.009	**0.039**	**0.074**	**0.096**	**0.100**	**0.052**	**0.083**	0.040	**0.050**
Ebro R. Tortosa	T_w	20.4	15.6	11.6	9.3	9.7	12.2	15.5	18.3	22.0	24.4	25.1	23.9	17.3
9981A-Tortosa	T_a	18.6	13.8	10.7	10.1	11.3	13.7	15.6	19.1	23.2	26.1	26.3	23.1	17.6
	ΔT_a	**0.044**	0.014	-0.019	0.000	-0.017	0.027	**0.064**	**0.078**	**0.080**	**0.048**	0.070	0.035	**0.040**

station and the downstream (Segre Serós and Cinca Fraga stations) and headwater (Segre Seo and Aragón Jaca stations) stations in the Cinca-Segre system, at least two months had significant upward trends ($P < 0.05$) in spring (Table 4). The highest values were at the Ebro Sástago station in June with an increase of 0.24 °C/year and the Ebro Ascó station with > 0.14 °C/year for all spring months (Table 4).

On the other hand, the period with fewer months with significant ΔT_w was autumn (October to December) (Table 4). In this season, all stations along the Ebro River had nonsignificant trends except Sástago and the last two stations, Xerta and Tortosa, in December (Table 4). In contrast, October trends were significant and high (0.09–0.12 °C/year) at the two stations on the Aragón River (Caparroso and Jaca), the mouth of the Segre River (Segre Serós station) and the Arba Tauste station, where the trend in November was also significant (Table 4).

During summer (July to September), only the stations on the Ebro River downstream of the Mequinenza Reservoir had significant trends for more than two months, with a peak at Ascó (in July, $\Delta T_w = 0.17$ °C/year). With respect to tributaries, the Cinca Fraga station was the only station that had significant trends in all summer months, reaching the highest value of the year (0.09–0.13 °C/year) (Table 4; Fig. 7).

Finally, in winter, the T_w trend showed similar behavior to the summer season. Only the stations below the Ascó NPP had more than two months with significant upward trends, especially the Ebro Ascó station, which had trends in the whole season above 0.14 °C/year. In winter, the Ebro Sástago station had two months with a significant trend, unlike summer, and among the stations downstream of the reservoirs, only Mequinenza had a significant trend in February. Other stations on the Ebro River with significant winter trends were those situated downstream of the Garoña NPP (Miranda and Haro), where January T_w increased by ~0.07 °C/year (Table 4). Among the tributary stations, only the Aragón Jaca and Cinca Fraga stations had a significant trend in March (Table 4; Fig. 7).

The stations located downstream of the NPPs (Ebro Miranda and Ebro Ascó stations) increased their ΔT_w in relation to the upstream stations (Ebro Cereceda and Ebro Flix stations) in all seasons except for autumn and summer at Miranda (Fig. 7). At Miranda, the ΔT_w was not significant from July to December, while at Ascó, only the months from October to December had nonsignificant trends (Table 4). The highest monthly ΔT_w in the basin was found at Ascó, where the ΔT_w was higher than 0.11 °C/year from January to September (Table 4), which entailed an increase in T_w of more than 5 °C during the study period (1980–2012). During summer and winter, the ΔT_w was nonsignificant for most months upstream of the Ascó NPP, but many months had significant and very high trends at the stations from Ascó downstream (Fig. 7), which were always lower at Xerta and Tortosa than at Ascó (Table 4).

Regarding the influence of the large reservoirs in the lower reaches, the Mequinenza and Flix stations did not have monthly ΔT_w as high as the upstream station (Ebro Sástago station) and the downstream station (Ebro Ascó station) in any season (Fig. 7). The monthly T_w trends were significant at Mequinenza only in February and May and at Flix from April to August (Table 4).

Generally, the monthly trends increased along the Ebro River in winter, spring and summer and were not as clear in autumn (Fig. 7). In the four seasons, the pattern of increasing monthly trends down the Ebro River was interrupted abruptly at Mequinenza, where the monthly ΔT_w was generally lower than that upstream (Sástago); this decrease in the ΔT_w along the river at Mequinenza was

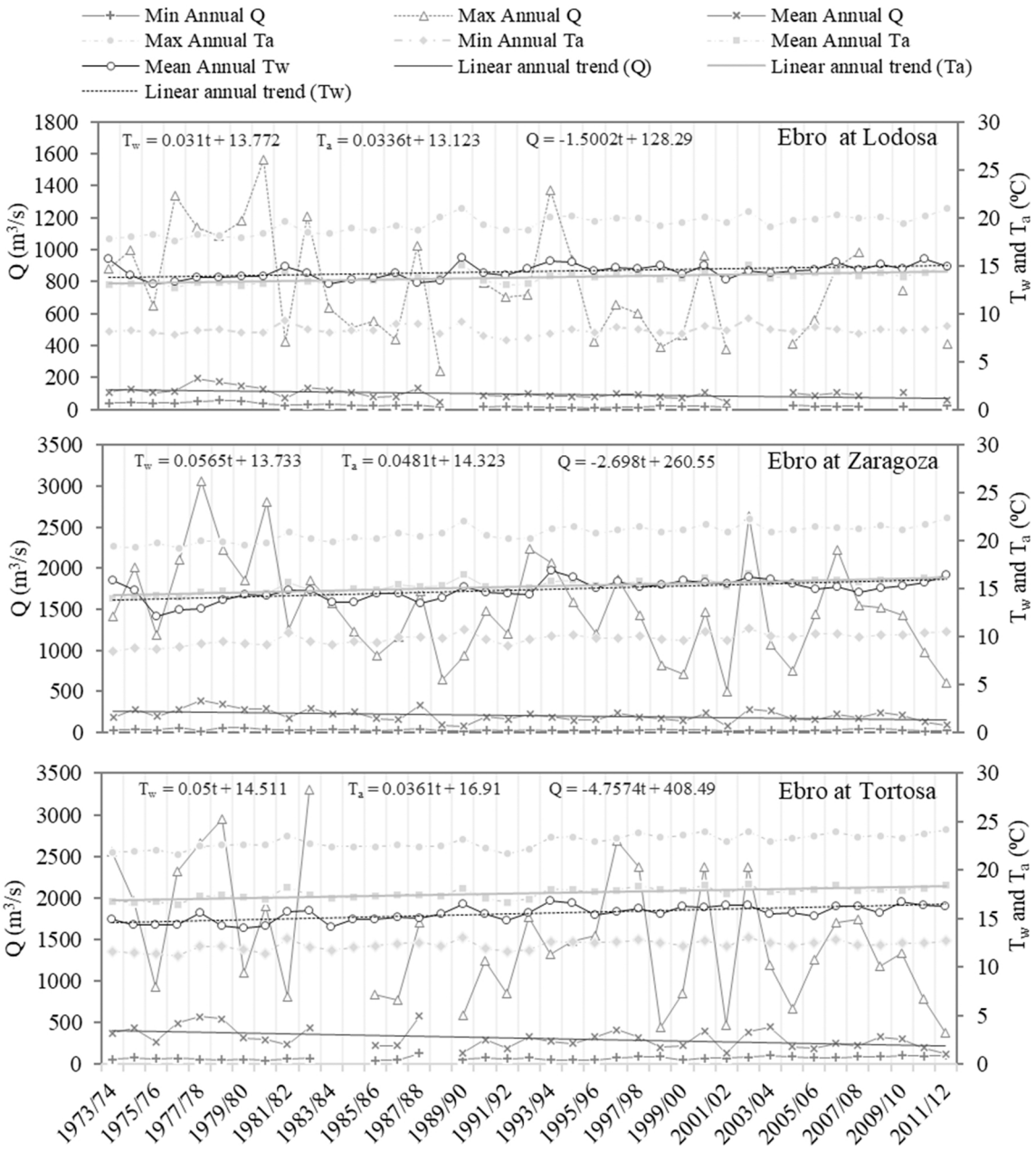

Fig. 6. Mean annual T_w (°C), mean annual T_a (°C) and mean annual flow (Q, m^3/s) in three stations at the Ebro River. The mean monthly minimum and maximum T_a and the maximum and minimum daily flow of the year are also included along with the linear regressions of T_w, T_a and flow on time. The T_a data series correspond to the Spanish Meteorological Agency (AEMET) stations at Logroño, Zaragoza and Tortosa (with the most complete T_a series close to the corresponding Ebro River stations).

less pronounced in winter (Fig. 7).

In spring, summer and winter, the trends in the tributary mouths were lower than the trends at the Ebro River stations upstream of their mouths except for the Cinca Fraga station in summer and winter (Fig. 7). In contrast, during autumn, the ΔT_w was higher in the tributaries than at the stations immediately upstream of their confluence (Fig. 7). The mouth stations of the Aragón-Arga system and the Arba River had significant trends mainly in spring and around October, whereas the Cinca-Segre system had a different behavior at its mouth, with no significant trends at the Segre Serós station (except for October) and significant trends mainly during summer and March-April at the Cinca Fraga station (Table 4; Fig. 7).

The seasonal T_w trends were similar to those present in Q_m and T_a in the 3 stations where these parameters were analyzed (Fig. 6, Table 5). The stations at the Ebro River (Lodosa, Zaragoza and Tortosa) showed a significant decrease in monthly flows, that were

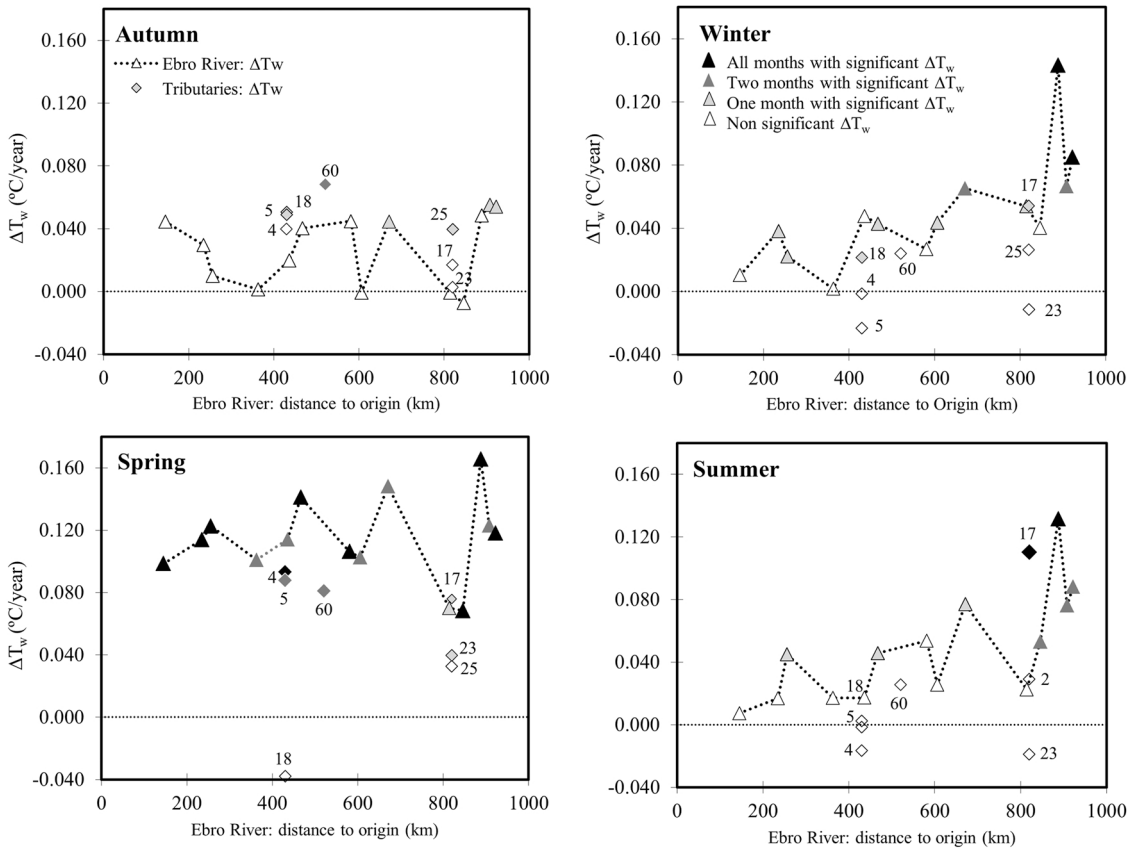

Fig. 7. Longitudinal profile of the mean seasonal ΔT_w (°C/year) along the Ebro River and main tributaries. The results obtained by the seasonal Mann Kendall test. The colors correspond to the number of months with a significant trend ($P<0.05$) in the season (from 0 to 3). The tributary stations are represented by the distance to the Ebro River origin of their discharge point. The numbers correspond to the tributary station codes (4 Arga Peralta; 5 Aragón Caparroso; 17 Cinca Fraga; 18 Aragón Jaca; 23 Segre Seo; 25 Segre Serós; and 60 Arba Tauste).

estimated from 1.9 to 17.8 Mm^3 /year from April to July. The only spring month without any significant flow trend was May (Table 5).

The meteorological stations analyzed (Logroño, Zaragoza and Tortosa) presented the same behaviors for T_a, with significant trends from 0.06 °C/year to 0.10 °C/year in all months from April to June. Except for Logroño in June, all these slopes were lower than the T_w trends at the closer quality stations (Table 4 and Table 5). October also showed an upward T_a trend in the 3 stations (Table 5), while it was a month in which no significant trend was observed in T_w in any station along the Ebro River (Table 4).

4. Discussion

All recent studies have noted a clear increase in air temperature in the last century that should affect water temperatures (IPCC, 2022). In this work, we found that T_w in the Ebro River has increased in most of the study stations over the last 40 years. It is difficult to define what part of these T_w changes should be attributed to the evolution of T_a and what part should be attributed to other factors, such as reservoir construction and management, increases in water consumption, land use changes (such as irrigation development) or thermal discharges, among others. Apparently, the behavior of T_w throughout the study period was not the result of any single specific environmental or anthropogenic change. It must have been a combination of all of them.

The T_w at the Ebro River stations with similar kinds of effects showed a common behavior.

The Mequinenza–Ribarroja–Flix reservoir system caused a decrease in the T_w annual range. At the downstream stations, the spring and summer T_w values decreased, while the autumn and winter T_w values increased. Dolz et al. (1996) also found differences of more than 5 °C in the mean T_w between the upstream reach of the Mequinenza Reservoir and downstream of the Flix Dam using continuous T_w measurements from June to July 1990. This lower-temperature water discharge from the Mequinenza Reservoir increased its temperature at a rate of 0.2 °C/km downstream (in the higher insolation hours) until the river regained its natural T_w.

Prats et al. (2010) measured T_w at 9 control stations along the lower reaches of the Ebro River (from the Mequinenza Reservoir to Xerta) and the Segre-Cinca River mouths from 1997 to 2003 (at 10-minute intervals). They found that the annual T_w range changed along this reach; the range was 3 °C smaller downstream of the reservoirs, with the temperature cycle lagging 20 days in relation to the upstream stations. They showed how T_w decreased in spring-summer with a maximum decrease of 3.5–4.0 °C in June-July and

increased in autumn-winter with a peak increase of 3.0–3.5 °C in November in relation to the nonaffected upper reaches. These authors also noted that the Cinca-Segre immediately upstream of the Ribarroja Reservoir contributed to the reservoir T_w stratification in spring and summer months and raised the T_w in the reservoir outflow. This could in turn have reduced the cooling ability of these waters upon the Ascó NPP effluents during summer.

In this study, similar results to those of Prats et al. (2010) were found at stations below reservoirs: the annual range at Flix (downstream of the reservoirs) was 3.2 °C lower than that at Sástago (upstream of the Mequinenza Reservoir). The summer mean T_w at the Flix station was 3.3 °C lower than that at Sástago, with maximum differences found in July (3.8 °C); and the autumn mean T_w at Flix was 2.5 °C higher, with maximum differences occurring in November (3.1 °C). Finally, this study showed that the maximum and minimum T_w at the downstream stations occurred one month later compared to the upstream stations.

It must be considered that the difference in T_w between the Sástago and Flix stations was not a consequence of the Mequinenza Reservoir regulation alone. The high flow discharge from the Cinca-Segre River (with lower mean T_w than the Ebro Mequinenza station) immediately upstream of the Ribarroja Reservoir also affected the T_w of the Ribarroja output. This difference was also higher because the Sástago station had a particularly high T_w range compared to other stations in the Ebro Depression. If the annual range at Flix is compared to the range at the Ebro River stations from Pignatelli to Pina (all of them located in the Ebro Depression, upstream of Sástago), the difference decreased to only 1.5 °C.

The reservoir system led to a decrease in T_w trends at downstream stations. Thus, the lowest annual trends were observed at the Ebro Flix ($\Delta T_w = 0.041$ °C/year) and Mequinenza stations ($\Delta T_w = 0.036$ °C/year).

Nuclear power plant discharges produced a significant increase in T_w. The highest increases were found during the summer months in the case of the Ascó NPP (2.7 °C), matching the lowest flow period. In the case of the Garoña NPP, the T_w increase was more homogeneous throughout the year, with higher values from August to December (>3 °C).

The different effects of the two NPPs on the Ebro River T_w patterns could be explained by the differences in streamflow and the effect of the Sobrón Reservoir. Streamflow was 6 times higher at the Ebro Ascó station than at the Ebro Miranda station.

Around the Ascó NPP, the highest flows in winter and spring (December to May) matched the lowest differences in T_w between the Flix and Ascó stations (Fig. 3d). In these months, the heat discharge from the Ascó NPP was absorbed by the Ebro River more easily, and thus, the difference in T_w between the two stations remained relatively low. The lower flow during the summer months in the Ebro River diminished the ability of the river to absorb the thermal discharges from the Ascó NPP, leading to higher differences during summer between the Flix and Ascó stations (Table 2; Fig. 3d).

The effects of the Ascó NPP on the Ebro River T_w was studied by Prats et al. (2010). These authors concluded that the discharges from this NPP increased the annual T_w by approximately 3 °C (1998–2003). The variability along the year depended on the Ebro River discharge (T_w increase was more noticeable in low flow periods) and additionally on the Ascó NPP management.

The mean T_w difference between the Ebro Flix and Ebro Ascó stations was 2.0 °C, with a higher difference from June to September (2.4–2.8 °C), coinciding with low Ebro River flows. The lower differences obtained in this work coincided with a longer T_w series (1975–2008) than in Prats et al. (2010), which took into account some cold T_w years before Ascó NPP activity.

Alberto and Arrúe (1986) estimated an increase in the Ebro River T_w of 3 °C associated with the Garoña NPP effluent (calculated from the NPP input and Ebro River flow). They observed that the flow-weighted mean T_w increased at Miranda from 9.3 °C before the start of the Garoña NPP (1960–1971) to 12.3 °C thereafter (1972–1982). They concluded that T_w in the river downstream of the Garoña NPP decreased by thermal dissipation (to water and air) and due to the thermal storage in the Sobrón Reservoir.

In this study, the difference in annual mean T_w between Cereceda and Miranda was 2.8 °C, half a degree higher than the difference observed by Alberto and Arrúe (1986) at the same stations (2.3 °C) from 1972 to 1982. This difference can be attributed to the T_w trends observed; the annual trend at Cereceda was lower than that at Miranda, thus increasing the difference in T_w between the two stations with time. Except for Garoña NPP effluents, there is no other plausible origin for the Ebro Miranda station high T_w (there are no high flowing tributaries, groundwater or urban main discharges, or large reservoirs). The water storage in the Sobrón Reservoir did not seem to be enough to absorb the Garoña heat effluent and to bring the Ebro River back to its natural T_w.

The highest annual T_w trend was observed at the Ebro Ascó station ($\Delta T_w = 0.12$ °C/year). This high value can only be explained by the NPP activity since 1985. However, it is important to mention that the temperature series at the Ebro Ascó station started in 1980, thus including 5 years with no discharges from the Ascó NPP. These first 5 years with lower T_w values may have led to the calculation of higher T_w trends. Excluding the first 5 years from the analysis, the annual trend was 0.08 °C/year and remained within the same range as the other lower Ebro River stations from Sástago to Tortosa except for the reservoir stations (Table 4).

Irrigation return flows produced an increase in T_w, but this behavior was not clear at all stations affected by the return flows from irrigated areas. The mean annual T_w and annual range at the Arba Tauste station were lower than those at other stations with similar climatic characteristics.

The Arba River Basin is located in a semiarid area in the middle Ebro Depression, and its headwaters do not originate from the Pyrenees but from the lower Pre-Pyrenean Range (Fig. 1). The Arba River is also the main collector of the irrigation return flows of the Bardenas Irrigation Scheme, which moved the maximum flow to the spring and summer period during the irrigation season (Fig. 3f). Additionally, the irrigation water for the Arba River Basin is diverted from the Aragón River at the Yesa Reservoir in the Aragón River headwaters (Fig. 1). This cold water was applied to the fields during the summer months, contributing to reducing the summer T_w and consequently to lessening the annual range (Fig. 3f).

Alberto and Arrúe (1986) found that the Arba Tauste station had higher thermal storage by unit mass than other stations in the surrounding area. They attributed this feature to the high flow during the irrigation season and not to warmer irrigation return flows. They attributed the different T_w between the Arba Tauste station and other stations to the supply of cool irrigation water and to the effects of evaporation and the cooling of the soils by irrigation water. It must be considered that most of the Arba irrigated land is flood

irrigated (78%) with low irrigation efficiency (62%) (Lorenzo-González, 2022).

Arga Peralta station had higher T_w in autumn and winter and lower T_w in summer than Aragón Caparroso station (Fig. 3g). In contrast with other tributaries, there is not much agricultural area in the Arga River Basin (5500 ha in 1999 (2%) and 10,700 ha in 2009 (4%); INE, 2009). In addition, there are no major reservoirs along the Arga River (only the minor Alloz (65 Mm^3) and Eugui (22 Mm^3) reservoirs in the headwaters), and the main populated areas (Pamplona) are located 90 km upstream of the Arga Peralta station. These natural features and the smaller anthropogenic effects in the Arga basin as compared with other tributary basins (Aragón, Cinca and Segre) may lead to lower temperature range and amplitude at its mouth.

The different ΔT_w values at the tributary mouth stations suggest a link between the T_w trend and irrigation development. Irrigated surfaces account for 16% and 28% of the total basin surface in the Cinca and Arba Rivers, respectively, with higher T_w increases, while irrigated land is 7% in the Aragón-Arga Basin and 10% in the Segre River Basin (irrigated land area elaborated with data from CHE, 2022) with lower T_w increases (Table 4).

The discharges of the main tributaries affected T_w in the Ebro River. The Aragón River inputs decreased the mean annual T_w and the annual temperature range in the Ebro River. However, this behavior changed between seasons and depended on the difference in T_w between the Ebro and Aragón Rivers and the flow ratios: T_w in the Ebro River decreased from summer to winter and increased in spring. Alberto and Arrúe (1986) found that the Aragón Jaca station and Yesa Reservoir had not attained a T_a–T_w equilibrium due to the high difference between T_a and T_w and to the high flow speed of this mountain river. These authors concluded that the storage time in the Yesa Reservoir was not enough to reach equilibrium in temperature and that the Aragón River probably would not reach this equilibrium all the way down to the mouth except in spring when the T_w in the Aragón River is similar or even higher than that at the Ebro Lodosa station. Furthermore, the Ebro River at the Aragón River discharge point had an abnormally high temperature produced by the Garoña NPP thermal effluent (as mentioned above) and did not reach T_a–T_w equilibrium for more than 150 km downstream from the Garoña NPP (Alberto and Arrúe, 1986).

The headwater stations (Aragón Jaca and Segre Seo), basically controlled by natural climate variability, exhibited a particular T_w behavior linked to snowmelt. For these stations, the increase in T_w during spring months (from April to June) was lower than that at the stations at the river mouths, which matched the higher thawing flows. Arrúe and Alberto (1986) found a relationship between flow and T_w that was unrelated to T_a on the Ebro River at Escatrón (close to the Sástago station). They attributed this relationship to episodes of river floods produced by snowmelt. Alberto and Arrúe (1986) found that the annual T_w in the Pyrenean headwaters was lower than T_a, with a difference of more than 1.5 °C at the Aragón Jaca station and in the Yesa Reservoir. This difference could also be observed at lower altitude stations as a result of the water origin and the high flow velocity in these kinds of rivers.

The best stations to analyze T_w effects by water diversion are located in the Ebro River lower reach at Xerta and Tortosa (14 km downstream). The Xerta Weir diverts more than 1200 Mm^3 /year at a high flow rate (>40 m^3/s) during the irrigation season (April to October). During summer, the Ebro River flow upstream of the Xerta Weir is approximately 200 m^3 /s, and it is in this period when abstraction effects should be more noticeable downstream of the weir, with a closer T_w–T_a relationship and an increase in T_w and T_a that should result in a higher annual range. Downstream of the Xerta Weir, the river would have less thermal capacity, lower flow velocity and higher residence time that would make the river more sensitive to summer high T_a. Nevertheless, the difference between stations was not particularly high, and missing data at the Ebro Xerta station in some years did not allow for a comparison between both stations.

In general, annual T_w trends increased from the upper reaches to the river mouths in the Ebro River and its tributaries, although some of these trends were nonsignificant (average of the mean annual significant trends was ~ 0.05 °C/year). There was also a clear seasonal behavior in the trends: the spring months had the highest significant trend (mean monthly ΔT_w ~ 0.10 °C/year) at most stations.

Bouza-Deaño et al. (2008) studied the trends (estimated by the seasonal Kendall slope estimator) of 34 chemical and physical parameters at 13 Ebro River stations from a shorter data series (1981–2004). They found a significant T_w increase at most stations with a mean trend of 0.08 °C/year. These authors found the highest ΔT_w at the Ebro Zaragoza station (0.18 °C/year, threefold the value found in this study: 0.05 °C/year), followed by Sástago (0.16 °C/year). These authors also found a clearly lower trend at the reservoir stations (0.03 °C/year) and higher increases downstream of the Ascó NPP (0.08 °C/year versus 0.12 °C/year in this work). These differences may be attributed to the different periods of the data series.

Alberto and Arrúe (1986) found for the lower Ebro River at Escatrón (close to Sástago) an increase of 0.08 °C/year for the annual flow weighed average T_w (1955–1978), and Prats et al. (2007), with a more complete data series (1955–2000), obtained an increase of 0.05 °C/year at the same station. It is difficult to compare this information with that obtained in this work at the Ebro Sástago station (0.08 °C/year) because of the different data periods. Nevertheless, the trends were significant in the three studies, indicating a persistent temperature increase since the 1950′s.

The general behavior in T_w could be related to the apparent flow trends in the Ebro River Basin: the highly regulated rivers had a decreasing trend in flow during spring and the increase in T_w was highest in spring. The progressive increase in the regulated flow in the Ebro River Basin during these years resulted in higher volumes of stored water in spring, decreasing the river flow. Lorenzo-Lacruz et al. (2012) found a decrease in discharge in more than 90% of the gauging stations in the Ebro River Basin following the increase in water consumption by agriculture and urban and industrial uses and the extension of natural vegetation in the basin headwaters at the expense of traditional agriculture (López-Moreno et al., 2011). Also, Álvarez-Cabria et al. (2016) applied a forest model to study the spatial and seasonal variability of water quality in the Ebro River Basin and found that an increase in forest cover reduced the mean annual T_w. The result has been an increase in T_w as more heat (resulting from rising T_a) must be absorbed by less water (resulting from lower flows). Lower flows also increase water travel times, which induces lower thermal inertia (Prats et al., 2010).

In this work, all stations along the Ebro River and especially the Ebro in Tortosa, showed a decreasing flow. The decrease in flows

matched the increase in T_w observed in the 1970′s to the 1990′s, pointing to a possible contribution of the flow decrease upon the T_w trends.

Additionally, global warming has induced a progressive decrease in snow storage in the Ebro River Basin in the last 50 years (MAGRAMA, 2008; López-Moreno and García-Ruiz, 2004).

In mountainous areas of the Ebro River Basin, the increase in T_a has led to a higher ratio of rainfall to snowfall, thus accelerating snowmelt (López-Moreno et al., 2011). The displacement of the peak melting flow to the early spring (IPCC, 2022; López-Moreno et al., 2011) and the progressive decrease in snow storage (MAGRAMA, 2008; López-Moreno and García-Ruiz, 2004) due to global warming also introduced less cold water during spring months. This effect is felt in the upper and middle Ebro River reaches, where the minimum T_w are found during the high flows originating from snowmelt (Arrúe and Alberto, 1986). Accordingly, the highest and most significant trends in T_w were found in the spring months.

5. Future tasks

The prognosis for the first half of the century in the Ebro River Basin is not promising. Air temperature is expected to increase by a mean of 1.5–1.6 °C with a maximum value in summer of 2.8 °C (MAGRAMA, 2010); and precipitation, although there has been no clear trend in recent decades (De Castro et al., 2005; López-Moreno et al., 2011; García Vera et al., 2002), is supposed to decrease between 3% and 4% (MAGRAMA, 2010). In this context, the Ebro River semiarid reaches with low flow velocity, less area protected by riparian vegetation and a large, exposed surface would experience the highest T_w increases due to climate change.

The analysis of river flows is also important. Many of the natural and anthropogenic factors affecting T_w in the Ebro River (including climate change) may also be altered by the reduction in river discharge. There is an apparent relationship between the evolution of T_w in the Ebro River and its tributaries (rising trend) and the evolution of their flows (decreasing trend). Future studies may focus on elucidating how the changes in river flows interfere with the T_w–T_a relationship, how they affect the heat transport capacity of rivers, and how these changes may aggravate some T_w effects, such as urban or industrial thermal discharges. Furthermore, clear links were found between T_w and T_a at all stations, but the strength of this link is different at different stations, reaches of rivers, and regions in the basin (stations downstream of major dams, Pyrenean headwaters, etc.) Additional research should be conducted to establish the nature and causes of these differences.

There are other factors affecting the Ebro River T_w, such as the groundwater supply and its thermal characteristics. The right bank tributaries exert important T_w control due to this effect in the Ebro River Basin (Alberto and Arrúe, 1986). However, given that these rivers do not contribute high discharges to the Ebro River, they were not included in this study. These groundwater controls could be included at a further stage in the analysis of the Ebro River water temperature regime.

Further consideration may be given to the selection of the sampling hour and day within the month to obtain adequate readings close to the average T_w of the month. The continuous (15-minute interval) data of the SAICA network of the CHE (CHE, 2021b) provide substantial information at some stations to help in the selection of the right sampling time for T_w (Isidoro et al., 2013).

6. Conclusions

Along the Ebro River, the T_w regime is markedly influenced by the effluents of the Garoña and Ascó NPPs and the tampering effect of the Mequinenza–Ribarroja–Flix reservoir system. The larger tributaries on the left bank (Aragón-Arga and Cinca-Segre Rivers) also exert a noticeable influence. Compared to these factors, the influence of irrigation return flows and irrigation development on water temperature was low. The flow regime and climate change are also factors that have a clear influence on T_w, especially during spring.

The influence of T_a on T_w was more pronounced at the stations along the Ebro River Depression (Pignatelli to Sástago) and at the mouth of the main tributaries (Aragón, Arga, Arba, Segre and Cinca Rivers). This influence was lower at the stations affected by NPP effluents or downstream of the main reservoirs and in the Pyrenean headwaters (Aragón Jaca and Segre Seo stations). Water temperature was therefore better related to T_a in the lower reaches of rivers under natural conditions, where low summer flows coincided with the highest T_a, indicating that this relationship might be linked to the relationship between T_w and Q_m.

River flow showed a weaker relationship with T_w, but the pattern of the link between T_w and Q_m throughout the stations was similar to that of T_a–T_w. Lower T_w was linked to higher Q_m at all stations except the Arba Tauste station, the station in which summer flows were essentially dominated by irrigation return flows.

There was an average annual upward trend in T_w. Only the stations in the Pyrenean headwaters (Aragón Jaca and Segre Seo stations) and the Aragón Caparroso station did not show significant annual trends. The magnitude of this trend increased downstream along the Ebro River, with peak values at the NPP-affected stations and lower values at reservoir-affected stations.

Climate change and flow trends are also factors that must be considered in studying the seasonal behavior and trends of T_w. The decrease in spring flows due to increased river regulation has reduced the cooling effect of spring snowmelt, whereas global warming has accelerated the thawing process. These factors explained the seasonal T_w trend patterns: the monthly trends were highest and most significant during spring at all stations along the Ebro River. On the other hand, low and nonsignificant seasonal T_w trends were found in autumn except for the significant slopes found in the tributaries in October.

CRediT authorship contribution statement

Marian Lorenzo-González: Methodology, Formal analysis, Data curation, Writing – original draft. **Dolores Quilez**: Writing – review & editing, Supervision. **Daniel Isidoro**: Conceptualization, Methodology, Writing – review & editing, Supervision.

Declaration of Competing Interest

The authors declare that they have no known competing financial interests or personal relationships that could have appeared to influence the work reported in this paper.

Data availability

All the data used in this work was provided by the Ebro River Basin Authority and was retrieved from publicly available data sources.

Acknowledgements

Thanks are given to Confederación Hidrográfica del Ebro for providing all data series analyzed in this work. This research did not receive any specific grant from funding agencies in the public, commercial, or not-for-profit sectors.

References

Abaurrea, J., Asín, J., Cebrián, A.C., García-Vera, M.A., 2011. Trend analysis of water quality series based on regression models with correlated errors. J. Hydrol. 400, 341–352. https://doi.org/10.1016/j.jhydrol.2011.01.049.

AEMET, 2022. Climatic data from the Spanish Meteorology Agency (AEMET). Accessible at: ⟨https://opendata.aemet.es/centrodedescargas/inicio⟩ (last access: 01/02/2023).

Alberto, F. and Arrúe, J.L., 1986. Anomalías térmicas en algunos tramos de la red hidrográfica del Ebro. Anales de Aula Dei 18 (1–2), 91–113. Accessible at: ⟨http://hdl.handle.net/10261/13599⟩ (last access: 14/12/2022).

Alberto, F. and Navas, A., 1987. Caracterización de niveles de saturación en calcita dolomita y yeso en las aguas superficiales de la Cuenca del Ebro. Anales de Aula Dei 18 (3–4): 199–228. Accessible at: ⟨http://hdl.handle.net/10261/13433⟩ (last access: 14/12/2022).

Álvarez-Cabria, M., Barquín, J., Peñas, F.J., 2016. Modelling the spatial and seasonal variability of water quality for entire river networks: relationships with natural and anthropogenic factors. Sci. Total Environ. 545–546, 152–162. https://doi.org/10.1016/j.scitotenv.2015.12.109.

ANAV, 2012. Memoria Anual 2012. The Nuclear Association of Ascó and Valdellos II (ANAV). Accessible at: ⟨https://anav.es/app/uploads/2016/05/Memoria_ANAV_2012_castellano.pdf⟩ (last access: 14/12/2022).

Arbat-Bofill, M., Sánchez-Juny, M., Bladé, E., Niñerola, D., Dolz, J., 2014. Hydrodynamics of Ribarroja Reservoir (Ebro River, Spain): water temperature, water velocities and water age. River Flow. 2014, 1737–1744. https://doi.org/10.13140/2.1.3271.5522.

Arrúe, J.L. and Alberto, F., 1986. El régimen térmico de las aguas superficiales de la Cuenca del Ebro. Anales de Aula Dei 18 (1–2), 31–50. Accessible at: ⟨http://hdl.handle.net/10261/13545⟩ (last access: 14/12/2022).

Batalla, R.J., Gómez, C.M., Kondolf, G.M., 2004. Reservoir-induced hydrological changes in the Ebro River Basin (NE Spain. J. Hydrol. 290, 117–136. https://doi.org/10.1016/j.jhydrol.2003.12.002.

Bejarano, M.D., Marchamalo, M., García de Jalón, D., González del Tánago, M., 2010. Flow regime patterns and their controlling factors in the Ebro basin (Spain. J. Hydrol. 385, 323–335. https://doi.org/10.1016/j.jhydrol.2010.03.001.

Beschta, R.L., Taylor, R.L., 1988. Stream temperature increases and land use in a forested Oregon Watershed. Water Resour. Bull. 24 (No. 1), 19–25. https://doi.org/10.1111/j.1752-1688.1988.tb00875.x.

Bouza, R., 2006. Estudio y evolución espacio-temporal de tendencias en datos históricos de calidad de aguas. Aplicación a la Cuenca Hidrográfica del Ebro. Ph. D. Dissertation. Sevilla University - Faculty of Chemistry. Sevilla (Spain). Accessible at: ⟨http://hdl.handle.net/11441/16009⟩ (last access: 14/12/2022).

Bouza-Deaño, R., Ternero-Rodriguez, M., Fernández-Espinosa, A.J., 2008. Trend study and assessment of Surface water quality in the Ebro River. J. Hydrol. 361, 227–239. https://doi.org/10.1016/j.jhydrol.2008.07.048.

Catalán, J. and Catalán, J.M., 1987. Ríos, caracterización y calidad de sus aguas. Bellisco, Madrid.

CHE, 2021b. Automatic Water Quality Information System (SAICA). Accessible at: ⟨https://saica.chebro.es/⟩ (last access: 02/11/2022).

CHE, 2021a. Water quality consulting, Ebro River Basin Authority (CHE). Accessible at: ⟨https://www.chebro.es/web/guest/resultados-anal%C3%ADticos⟩ (last access: 02/11/2022).

CHE, 2008. The Ebro River Management Plant from Martin River to the river mouth, previously document for the Ebro Management Plant analysis. Ebro River Basin Authority (CHE). Accessible at: ⟨https://www.chebro.es/web/guest/informes-de-nuestros-rios⟩ (last access: 02/11/2022).

CHE, 2012. Evolución del pH y de la temperatura del agua en los ríos de la Cuenca del Ebro. Ebro River Basin Authority (CHE).

CHE, 2022. Proyecto de Plan Hidrológico de la Demarcación Hidrográfica del Ebro. Revisión de Tercer Ciclo (2022–2027). Ebro River Basin Authority (CHE). Accessible at: ⟨https://www.chebro.es/web/guest/proyecto-de-plan-hidrologico⟩ (last access: 02/11/2022).

Coll, L., López de Santa María, J. and Fernández, A., 1996. Perspectiva Histórica. Revista de la Sociedad Nuclear Española, No. 159. Accessible at: ⟨https://www.revistanuclear.es/hemeroteca/?sf-s=&sf-att-120-lk=Coll&sf-att-144-lk=&sf-att-122-eq=&sf-att-119-eq=1996&sf-shortcode=2253⟩ (last access: 02/11/2022).

De Castro, M., Martín-Vide, J. and Alonso, S., 2005. The climate of Spain: Past, present and scenarios for the 21st century. Ministerio de Medio Ambiente: A preliminary general assessment of the impacts in Spain due to the effects of climate change. Accessible at: ⟨https://www.miteco.gob.es/es/cambio-climatico/temas/impactos-vulnerabilidad-y-adaptacion/preliminary_assessment_impacts_2005_tcm30–178514.pdf⟩ (last access: 02/11/2022).

Diamantini, E., Lutz, S.R., Malluci, S., Majone, B., Merz, R., Bellin, A., 2018. Driver detection of water quality trends in three large European River Basin. Sci. Total Environ. 612, 49–62. https://doi.org/10.1016/j.scitotenv.2017.08.172.

Dolz, J., Puertas, J., Herrero, E., 1996. Incidencias de los embalses en el comportamiento térmico del río. In J. Dolz, J. Puertas, A. Aguado and L. Agulló, 1996. Efectos térmicos en presas y embalses. Colegio de Ingenieros de Caminos, Canales y Puertos. Madrid, pp. 9–25.

EEA, 2017. Climate change impacts and vulnerability in Europe 2016. An indicator-based report European Environmental Agency, Report No 1/2017. Accessible at: ⟨https://www.eea.europa.eu/publications/climate-change-impacts-and-vulnerability-2016⟩ (last access: 02/11/2022).

García de Jalón, D., 1996. Impactos de las modificaciones del régimen térmico en las comunidades fluviales. In J. Dolz, J. Puertas, A. Aguado and L. Agulló, 1996. Efectos térmicos en presas y embalses. Colegio de Ingenieros de Caminos, Canales y Puertos. Madrid, pp. 95–107.

Fazel, N., Torabi Haghighi, A., Kløve, B., 2017. Analysis of land use and climate change impacts by comparing river flow records for headwaters and lowland reaches. Glob. Planet. Change 158, 47–56. https://doi.org/10.1016/j.gloplacha.2017.09.014.

García de Jalón, D., Montes, C., Barceló, E., Casado, C., Menes, F., 1988. Effects of a hydroelectric regulation scheme on fluvial ecosystems within the Spanish Pyrenees. Regul. River Res. Manag. 2 (4), 479–491. https://doi.org/10.1002/rrr.3450020402.

García Vera, M.A., 2013. The application of hydrological planning as a climate change adaptation tool in the Ebro basin. Int. J. Water Resour. Dev. 29 (No. 2), 219–239. https://doi.org/10.1080/07900627.2012.747128.

García Vera, M.A., Abaurrea, J., Asín Lafuente, J. and Centelles Nogues, A., 2002. Evolución de las precipitaciones en la cuenca del Ebro: caracterización espacial y análisis de tendencias. VII Reunión Nacional de Climatología, Albarracín 2002 (Spain). Accesible at: ⟨https://www.researchgate.net/publication/264352491_Evolucion_de_las_precipitaciones_en_la_cuenca_del_Ebro_caracterizacion_espacial_y_analisis_de_tendencias⟩ (last access: 02/11/2022).

Gilbert R.O., 1987. Statistical methods for environmental pollution monitoring. Van Nostrand Reinhold Ed. New York.
Gusarov, A.V., 2019. The impact of contemporary changes in climate and land use/cover on tendencies in water flow, suspended sediment yield and erosion intensity in the northeastern part of the Don River basin, SW European Russia. Environ. Res. 175, 468–488. https://doi.org/10.1016/j.envres.2019.03.057.
Hirsch, R.M., Slack, J.R., Smith, R.A., 1982. Techniques of trend analysis for monthly water quality data. Water Resour. Res. 18 (1), 107–121. https://doi.org/10.1029/WR018i001p00107.
INE, 2009. National Statistics Institute. Agriculture Census. Accessible at: ⟨https://www.ine.es/dyngs/INEbase/es/operacion.htm?c=Estadistica_C&cid=1254736176851&menu=resultados&idp=1254735727106⟩ (last access: 02/11/2022).
IPCC, 2022. Climate Change 2022: Impacts, Adaptation and Vulnerability Working Group II Contribution to the Sixth Assessment Report of the Intergovernmental Panel on Climate Change. Accessible at: ⟨https://www.ipcc.ch/report/ar6/wg2/downloads⟩ (last access: 02/11/2022).
Isaak, D., Wollrab, J.S., Horan, D., Chandler, G., 2011. Climate change on stream and river temperatures across the northwest U.S. from 1980-2009 and implications for salmonid fishes. Clim. Change 113, 499–524. https://doi.org/10.1007/s10584-011-0326-z.
Isidoro, D., Balcells, M., Clavería, I., and Dechmi, F., 2013. Momento óptimo de muestreo en las estimas de las cargas de contaminantes en el río Alcanadre (Huesca), XXXI Congreso Nacional de Riegos; Orihuela, 18–20 de junio de 2013. Accessible at: ⟨http://hdl.handle.net/10261/79028⟩ (last access: 02/11/2022).
Kaushal, S.S., Likens, G.E., Jaworski, N.A., Pace, M.L., Sides, A.M., Seekell, D., Belt, K.T., Secor, D.H., Wingate, R.L., 2010. Rising stream and river temperatures in United States. Front. Ecol. Environ. 8 (9), 461–466. https://doi.org/10.1890/090037.
Kendall, M.G., 1975. Rank Correlation Methods, 4th Ed. Charles Griffin, London.
Kinouchi, T., Yagi, H., Miyamoto, M., 2007. Increase in stream temperature related to anthropogenic heat input from urban wastewater. J. Hydrol. 335 (1–2), 78–88. https://doi.org/10.1016/j.jhydrol.2006.11.002.
Labrador-Páez, L., Mingoes, C., Jaque, F., Haro-González, P., Bazin, H., Zwier, J.M., Jaque, D., Hildebrandt, N., 2019. pH dependence of water anomaly temperature investigated by Eu (III) cryptate luminescence. Anal. Bioanal. Chem. https://doi.org/10.1007/s00216-019-02215-0.
López-Moreno, J.I., García-Ruiz, J.M., 2004. Influence of snow accumulation and snowmelt processes on the distribution on streamflow in the central Spanish Pyrenees. Hydrol. Sci. J. 49, 787–802. https://doi.org/10.1623/hysj.49.5.787.55135.
López-Moreno, J.I., Vicente-Serrano, S.M., Moran-Tejeda, E., Zabalza, J., Lorenzo-Lacruz, J., García Ruiz, J.M., 2011. Impact of climate evolution and land use changes on water yield in the Ebro Basin. Hydrol. Earth Syst. Sci. 15, 311–322. https://doi.org/10.5194/hess-15-311-2011.
Lorenzo-González, M.A., 2022. Regadío y calidad fisico-química de las aguas superficiales en la Cuenca del Ebro. Ph. D. Dissertation. University, Zaragoza (Spain).
Lorenzo-González, M.A., Isidoro, D., Quílez, D., 2014. Long term salinity trends in the Ebro River (Spain). 3rd Salinity Forum. University of California Riverside, USA.
Lorenzo-Lacruz, J., Vicente-Serrano, S.M., López-Moreno, J.I., Morán-Tejada, E., Zabalza, J., 2012. Recent trends in Iberian streamflow (1945-2005). J. Hydrol. 414–415, 463–475. https://doi.org/10.1016/j.jhydrol.2011.11.023.
MAGRAMA, 2008. Datos sobre la nieve y los glaciares en las cordilleras españolas, Programa ERHIN (1984–2008). Ministerio de Medio Ambiente y Medio Rural y Marino de España. Accessible at: ⟨https://www.miteco.gob.es/es/agua/publicaciones/ERHIN_publicaciones_documentacion.aspx⟩ (last access: 02/11/2022).
MAGRAMA, 2010. Estudio de los impactos del cambio climático en los recursos hídricos y las masas de agua. Ministerio de Medio Ambiente y Medio Rural y Marino (MAGRAMA) and Centro de Estudios de Experimentación de Obras Públicas (CEDEX). Accessible at: ⟨https://www.miteco.gob.es/en/agua/temas/planificacion-hidrologica/planificacion-hidrologica/EGest_CC_RH.aspx⟩ (last access: 02/11/2022).
MAGRAMA, 2021. Anuario de Aforos, Ministerio de Medio Ambiente y Medio Rural y Marino (MAGRAMA). Accessible at: ⟨https://sig.mapama.gob.es/redes-seguimiento/⟩ (last access: 02/11/2022).
Mann, H.B., 1945. Non-Parametric tests against trend. Econometrica 13 (No. 3), 245–259. https://doi.org/10.2307/1907187.
Masachs, V., 1948. El Régimen de los ríos Peninsulares. Consejo Superior de Investigaciones Científicas: Instituto Lucas Mallada de Investigaciones Geológicas, Barcelona.
MOPU, 1990. Análisis de Calidad de Aguas, Red Oficial del Ministerio de Obras Públicas y Urbanismo, Dirección General de Obras Hidráulicas, años del 1973/74 al 1989/90, Madrid.
Nebeker, A.V., 1971. Effect of high winter water temperatures on adult emergence of aquatic insect. Water Res. 5, 777–783. https://doi.org/10.1016/0043-1354(71)90100-X.
NUCLENOR, 2013. Central Nuclear de Santa María de Garoña, Datos y Cifras. Accessible at: ⟨https://www.nuclenor.org/public/otros/cnsg_datos_cifras.pdf⟩ (last access: 02/11/2022).
Peterson, D.E. and Jaske, R.T., 1968. A test simulation of potential effects of thermal power plants on stream on the upper Mississippi River Basin, Battelle Memorial Institute Pacific Northwest Laoratory Richland, Washington. Accessible at: ⟨https://www.osti.gov/servlets/purl/4809113⟩ (last access: 02/11/2022).
Poole, G.C., Berman, C.H., 2001. An ecological Perspective on in-stream temperature: natural heat dynamics and mechanism of human-caused thermal degradation. Environ. Manag. 27 (6), 787–802. https://doi.org/10.1007/s002670010188.
Prats, J., 2011. El règim tèrmic del tram inferior de lEbre i les seues alteracions. Ph. D. Dissertation. Polytechnic University of Catalonia, Barcelona. Accessible at: ⟨http://hdl.handle.net/10803/96154⟩ (last access: 02/11/2022).
Prats, J., 2012. Water temperature modeling in the Lower Ebro River (Spain): heat fluxes, equilibrium, temperature, and magnitude of alteration caused by reservoir and thermal effluent (Article number). Water Resour. Res. 48 (5), W05523. https://doi.org/10.1029/2011WR010379.
Prats, J., Val, R., Armengol, J., Dolz, J., 2007. A methodological approach to the reconstruction of the 1949-2000 water temperature series in the Ebro River at Escatrón. Limmetica 26 (2), 293–306. https://doi.org/10.23818/limn.26.25.
Prats, J., Val, R., Armengol, J., Dolz, J., 2010. Temporal variability in the thermal regime of the lower Ebro River (Spain) and alteration due to anthropogenic factors. J. Hydrol. 387, 105–118. https://doi.org/10.1016/j.jhydrol.2010.04.002.
Schmidt-Nielsen, K., 1997. Animal Physiology: Adaptation and Environment. Cambridge University Press, Cambridge.
Stevens, H.H., Ficke, J.F., and Smooth, G.F., 1975. Water temperature influential factors, field measurement and data presentation. Techniques of Water Resource Investigation of the United State Geological Survey, Book No. 1, Chapter D1. ⟨https://doi.org/10.3133/twri01D1⟩.
Stumm, W., Morgan, J.J., 1970. Aquatic Chemistry. An Introduction Emphasizing Chemical Equilibria in Natural Waters. Wiley-Interscience Ed. https://doi.org/10.1021/ed048pA779.1.
Val, J., Chinarro, D., Pino, M.R., Navarro, E., 2016. Global change impacts on river ecosystems: a high-resolution watershed study of Ebro River metabolism. Sci. Total Environ. 569–570, 774–883. https://doi.org/10.1016/j.scitotenv.2016.06.098.
Val, J., Pino, M.R., Chinarro, D., 2018. Development of a new methodology for the creation of water temperature scenarios using frequency analysis tool. Sci. Total Environ. 618, 610–620. https://doi.org/10.1016/j.scitotenv.2017.06.064.
Val, R., Niñerola, D., Armengol, J., Dolz, J., 2003. Incidencias de los embalses en el régimen térmico del río. El caso del tramo final del Ebro. Limnética 22 (1–2), 85–92. https://doi.org/10.23818/limn.22.05.
Valencia, J.L., 2007. Estudio estadístico de la calidad de las aguas de la Cuenca del Hidrográfica del río Ebro. Ph. D. Dissertation. Technical University of Madrid, School of Agricultural, Food and Biosystems Engineering, Madrid. ⟨https://doi.org/10.20868/UPM.thesis.454⟩.
Vannote, R.L., Sweeney, B.W., 1980. Geographic analysis of thermal equilibria: a conceptual model for evaluating the effect of natural and modified thermal regimes on aquatic insect communities. Am. Nat. 115, 667–695. ⟨https://www.jstor.org/stable/2460685⟩. last access: 02/11/2022.
Verma, R.D., 1986. Environment Impacts of Irrigation projects. J. Irrig. Drain. Eng. 112 (4), 322–330. https://doi.org/10.1061/(ASCE)0733-9437(1986)112:4(322).
Ward, J.V., Stanford, J.A., 1982. Thermal responses in the evolutionary Ecology of aquatic insect. Annu. Rev. Entomol. 27, 97–117. https://doi.org/10.1146/annurev.en.27.010182.000525.
Webb, B.W., 1996. Trends in stream and river temperature. Hydrol. Process. 10, 205–226. https://doi.org/10.1002/(SICI)1099-1085(199602)10:2<205::AID-HYP358>3.0.CO;2-1.
Webb, B.W., Nobilis, F., 1995. Long term water temperature trends in Austrian rivers. Hydrol. Sci. J. 40 (1), 83–96. https://doi.org/10.1080/02626669509491392.

Webb, B.W., Nobilis, F., 2007. Long-term changes in river temperature and the influence of climatic and hydrological factors. Hydrol. Sci. J. 52 (1), 74–85. https://doi.org/10.1623/hysj.52.1.74.

Webb, B.W., Walling, D.E., 1988. Modification of temperature behavior through regulation of a British river system. Regul. River Res. Manag. 2 (2), 103–116. https://doi.org/10.1002/rrr.3450020205.

WHO, 2022. World Guidelines for Drinking-water Quality, Fourth Edition Incorporating the First and Second Addenda. World Health Organization, 583 p. Accessible at: ⟨https://www.who.int/publications/i/item/9789240045064⟩ (last access: 02/11/2022).